2011

Avian Cerebellum Specialization in Relation to Acrobatic Courtship Displays in Manakins (Pipridae)

Steven Ray Wilkening

AVIAN CEREBELLUM SPECIALIZATION IN RELATION TO ACROBATIC COURTSHIP DISPLAYS IN MANAKINS (PIPRIDAE)

A Thesis
presented in partial fulfillment of requirements
for the degree of Master of Science
in the Department of Biology
The University of Mississippi

by

Steven R. Wilkening

May 2011

ABSTRACT

The courtship displays of male manakins (Pipridae) involve an array of acrobatic and postural elements. Previously it was found that species with elaborate displays exhibit specializations in motor planning and coordination areas of the brain. Several studies have suggested a relationship between cerebellum (Cb) morphology and distinct motor-related functions for the anterior Cb (somatosensory, flying, hopping/walking), posterior Cb (vision, audition, flying, hopping/walking), and vestibular Cb (flying, hopping/walking, vestibular). The anterior, posterior and vestibular Cb as well as basic morphological features of the Cb were measured and tested for a relationship with courtship display complexity in manakins. I compared Cb morphology of four species of manakins: *Manacus vitellinus*, *Pipra mentalis*, *Chiroxiphia lanceolata*, and *Lepidothrix coronata* as well as one species of flycatcher, *Mionectes oleagineus*, representing a range of display complexities. I scored each species's display for overall complexity, taking into account acrobatic elements, sound production by the wings and level of coordination between two displaying males. The following features of Cb morphology were measured: Cb volume, white matter volume, molecular layer volume, granular layer volume, volume of the lateral cerebellar nucleus (CbL), volume of the medial cerebellar nucleus (CbM), CbL cell density, CbM cell density, Purkinje cell (PC) size and density, and the sizes of the anterior Cb, posterior Cb and vestibular Cb cortices. Morphology variables were corrected for allometry, if necessary. Parallel analyses were performed on data corrected for phylogenetic

relatedness using independent contrasts and on non-corrected data. Data reduction was accomplished by performing individual linear regressions of each Cb morphology variable vs. display complexity were performed, and variables for which $p<0.1$ (CbM volume, vestibular Cb size, white matter volume and PC size for both phylogenetically corrected data and non-corrected data) were then tested in stepwise multiple regressions. For non-corrected data, both vestibular Cb size (negative relationship) and CbM volume (positive relationship) best predict display complexity. For phylogenetically corrected data, only white matter volume predicted display complexity (positive relationship). This study is the first to provide evidence that specific morphological features of the Cb may evolve in conjunction with a sexually selected behavior.

LIST OF ABBREVIATIONS

Cb	cerebellum
CbL	lateral cerebellar nucleus
CbM	medial cerebellar nucleus
CFI	cerebellar foliation index
FOV	field-of-view
GLM	general linear model
NBF	10% neutral-buffered formalin
PBS	0.1M phosphate-buffered saline
PC	Purkinje cell

ACKNOWLEDGMENTS

I would like to thank my advisor, Dr. Lainy Day, for dedicating so much of her time to assisting me with the project. I thank my committee members, Dr. Gary Gaston, Dr. Brice Noonan, and Dr. Karen Sabol for their time and patience in facilitating completion of my master's degree. I appreciate the hard work from field assistants Sonja Gaessler and Jed Brensinger in helping to collect birds. I also thank my lab assistant John Ball for helping with morphology measurements and constructing drawings of the manakin displays. I would like to thank the Microtechniques course students for helping with hematoxylin and eosin staining. The University of Mississippi Biology Department staff and faculty as well as the staff at the Graduate School were extremely helpful, and I appreciate their assistance. I would also like to thank the Smithsonian Tropical Research Institute for authorizing this work and providing lab facilities in Panama, as well as Autoridad Nacional del Ambiente de Panama for approving this work and Autoridad del Canal de Panama for allowing me to collect specimens on their land. Funding was provided by The University of Mississippi Graduate Student Council, a grant from the UM College of Liberal Arts to Dr. Lainy Day, and NSF grant #0646459 to Dr. Barney Schlinger, PI, and Dr. Lainy Day, Senior Personnel.

TABLE OF CONTENTS

LIST OF TABLES

LIST OF FIGURES

I. INTRODUCTION

The primary goal of this research was to determine whether there are morphological adaptations in the brains of manakins (Pipridae), a group of suboscine Passeriform birds, relating to the elaborate acrobatic courtship displays that they perform. Specifically, I examined the relationship between these displays and the cerebellum (Cb), a brain region with functions that suggest that it is likely to be important in the acquisition and/or performance of manakin displays. I used a comparative method to determine if there is a relationship between the Cb and manakin displays. Each species of manakin in this study has a display that is quite distinct from that of other species. These species differ in the types and complexities of movements, flights, postures, mechanical sounds, and social interactions involved in their displays. Although the Cb has recently been shown to play a role in birdsong (DiGuisto & Day, unpublished data), manakins do not learn songs, and their vocalizations are neither complex nor thought to be under strong selection. Therefore, comparing features of the Cb between species with different display complexities may reveal which features of the Cb are related to the ability to perform complex displays. The specific features that I compared are the total Cb volume; granular layer volume; molecular layer volume; white matter volume; size of anterior, posterior, and vestibular Cb cortices; size of Purkinje cells (PCs), linear density of PCs; volume of the medial and lateral cerebellar nuclei (CbM and CbL, respectively); and cell density in CbM and CbL.

I tested the hypothesis that there is an association between display complexity and in Cb morphology. Each species was given a display complexity score based on the overall complexity of their display behavior. According to the principle of proper mass (Jerison 1973), if an association exists between Cb and behavior, the species with more complex displays should exhibit larger Cb regions or greater cell density than species with less complex displays. Therefore, in analyses of four manakin species and a tyrant flycatcher (a closely related, lekking non-manakin) that exhibit species-level variation in complexity of courtship displays, I expected a positive correlation between Cb size and display complexity for each portion of the Cb involved in the courtship displays with the exception that allometric scaling might necessitate the expansion of some features with shrinkage of others. Phylogenetic inertia—the tendency for a trait to be more similar in closely related species than in distantly related species, even with no selective force acting on the trait—could be a factor influencing display complexity or Cb morphology trends. Therefore, I used independent contrasts to correct for phylogenetic relatedness. The Cb morphology features found to be correlated with display complexity were then tested in a stepwise multiple regression model to determine which variables most likely explain variation in display complexity. I predicted that Cb volume, PC size and density, and CbM and CbL volume and cell density will be positively correlated with increasing display complexity since PC and CbM/L reflect major functions and are convergence points for inputs and outputs in the Cb.

i. BRAIN SPECIALIZATIONS

The vertebrate brain has localized functional regions. Specific behaviors can be strongly associated with the activity of these particular regions, and prevalence of a

behavior may be related to increased cell numbers in and size of the associated region. Regions of the brain responsible for behaviors or functions more prevalent in one organism than another should be larger in the former (Jerison 1973). For example, somatosensory representation in the brain for unique, receptor-dense tactile appendages in the star-nosed mole is localized and greatly increased in size relative to that for other senses (Catania & Kaas 1995). The size of the hippocampus has been shown to be proportional to use in spatial learning in mammals, birds and reptiles (reviewed in: Sherry et al. 1992; Day 2003). The pretectal nucleus lentiformis mesencephali, which is involved in gaze stabilization in vertebrates, is enlarged in a group of birds (hummingbirds; Trochilidae) that use gaze stabilization to hover in flight versus non-hovering birds (Iwaniuk & Wylie 2007). Similarly, the auditory midbrain nucleus, which integrates auditory input for sound localization, is enlarged in owls (Strigiformes), which primarily use sound cues to hunt prey at night (Iwaniuk et al. 2006b).

A relationship also exists between courtship behaviors arising evolutionarily through sexual selection and their related brain regions. Because female birds carry the burden of egg-laying, limiting their maximum potential number of offspring and increasing their investment in reproduction relative to males, the theoretical benefit to a female's lifetime reproductive success is maximized by further investing her time and energy into the rearing of her offspring. Hence, a male is free to invest his time and energy in strategies that lead to a greater number of females mating with him rather than caring for his individual offspring. Because of this greater investment in fewer offspring by females, and the large number of males willing to mate with nearly any female, a female has the privilege of choosing with whom she mates. Females judge male quality by observing specific traits,

which are often advertised by the male in a courtship display. Those males that excel at the display behavior get to mate and pass their genes and traits on to offspring, while other males may not obtain any offspring. Presumably, these traits reflect a male's quality in terms of health and social status. Therefore, over many generations, these male traits evolve and diverge from those of females, and may become quite exaggerated. If extensive neural processing underlies the display behavior, the nervous system may become specialized over evolutionary time.

In many species of oscine (Passeriformes, passeri) birds, males learn particular songs that they sing to females in order to attract and convince them to mate. There exist unique brain regions related to the learning and production of song. The size of the major song learning region, HVC, is positively correlated with song syllable repertoire size both within and among songbird families (Devoogd et al. 1993; Szekely et al. 1996). The sizes of three song regions, including HVC, are greater in males that sing than in females that do not sing in several species including canaries and zebra finches (e.g. Nottebohm & Arnold 1976; Brenowitz et al. 1997). One group of oscines, the bowerbirds (Ptilonorhynchidae), not only learn vocalizations and have related song circuitry, but also construct complex display "bowers". Males build these elaborate bowers out of sticks or grasses and decorate with insects, flowers, fruits and other objects and use these bowers to attract mates. The building of these bowers requires procedural learning, planning and performance of stereotyped postures and movements, and the size of the Cb across five species of bowerbird relates to the complexity of the bower that the species builds (Day et al. 2005). This relationship demonstrates that the Cb is subject to the force of sexual selection and suggests that sexual selection for complex motor displays in manakins may affect Cb size.

ii. MANAKIN OVERVIEW

Several species of manakins perform acrobatic courtship displays that may correspond to specializations of particular brain regions. While the manakin displays are distinct from those of bowerbirds, the presence of common elements such as intensive motor planning and performance of stereotyped movements and postures raises the possibility that the manakins may also have evolved neurological specializations in the Cb independently of bowerbirds. The manakins inhabit neotropical forests and are nearly all sexually dimorphic lekking birds. A lek breeding system is one in which females freely choose their mates among males located in close proximity to one another—in a "lek"—and the males never assist with raising offspring (Bradbury 1981). In addition to acrobatic and postural elements, displays of many manakin species include mechanical sounds produced by extremely rapid and forceful movements of the wings and also include male-male cooperation in some species. The complexity of display elements and types of acrobatics performed, if any, depend on the species.

While progress has been made in understanding the hormonal regulation of display behaviors in the golden-collared manakin, *Manacus vitellinus*, (Schlinger et al. 2001; Day et al. 2007; Schlinger et al. 2008), virtually nothing is known about neural adaptations related to manakin displays. One would expect, given the uniqueness of most manakin species' displays, that there exist specializations in brain regions that control these physical behaviors. Because the displays are acrobatic in nature, one would expect specializations to exist in a region involved in learning, planning, and coordination of complex motor movements such as the Cb. The Cb is also involved in aspects of motor cognition (Fuentes & Bastian 2007; Glickstein et al. 2009), as well as in learning-by-observation of stereotyped

procedural movements such as those performed during bowerbird displays (Day et al. 2005; Torriero et al. 2007). Below I describe the display of each manakin species included in this study and the neuroanatomical features of the Cb that are predicted to be most important to these displays.

iii. MANAKIN DISPLAY DESCRIPTIONS

Four species of manakins and one flycatcher were examined in this study: golden-collared manakin (*Manacus vitellinus*), red-capped manakin (*Pipra mentalis*), lance-tailed manakin (*Chiroxiphia lanceolata*), blue-crowned manakin (*Lepidothrix coronata*), and ochre-bellied flycatcher (*Mionectes oleagineus*). Each of their displays are distinct from one another and also differ in complexity and types of elements included. The procedure for scoring display complexity is described in the Methods section (Table 2).

Golden-collared manakin (*M. vitellinus*) males are black and olive with a bright yellow collar and long, yellow "beard" feathers that the birds extend during a display. At the start of the breeding season, a male clears a patch of leaves on the forest floor in a circle ~0.5 m in diameter. Surrounding this "arena" are a few small vertical saplings. When displaying, a male perches on a vertical sapling with his body and beard extended in a precise posture. He then hops very rapidly between saplings in his arena, and in midair on each hop he snaps his wings behind his back to produce a loud firecracker sound, a "wingsnap," before alighting on the next sapling and righting his posture (Figure 1; Chapman 1935). To conclude the sequence of hops between saplings he often performs a back-flip from the sapling to the ground and then alights, producing a "grunt" sound with the wings (Fusani et al. 2007) and sliding down the sapling to mount a female if there is

one present (Figure 1 arrow b). Perched males also produce rapid "rollsnaps," wing snaps at ~5.6 Hz that are believed to be involved in territorial communication.

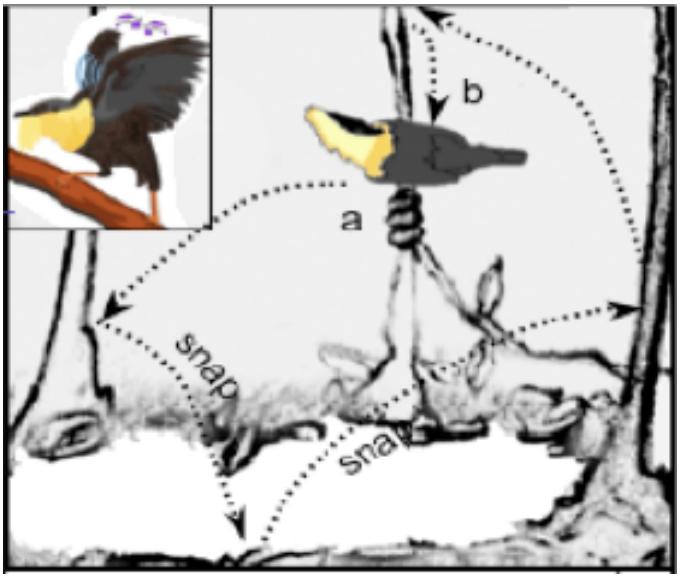

Figure 1. Depiction of *M. vitellinus* courtship display. Display largely consists of rapidly hopping between vertical saplings over a cleared court while making loud wingsnaps with each hop.

Red-capped manakin (*P. mentalis*) males are black with bright red heads and bright yellow-feathered legs. Males' displays consist of swooping flights in the lower canopy with non-vocal mechanical 'pop' noises upon landing. While perched on a branch, a male performs a "moonwalk" display in which tiny, rapid hops give the illusion that the bird is sliding backwards along a branch (Figure 2; Skutch 1969).

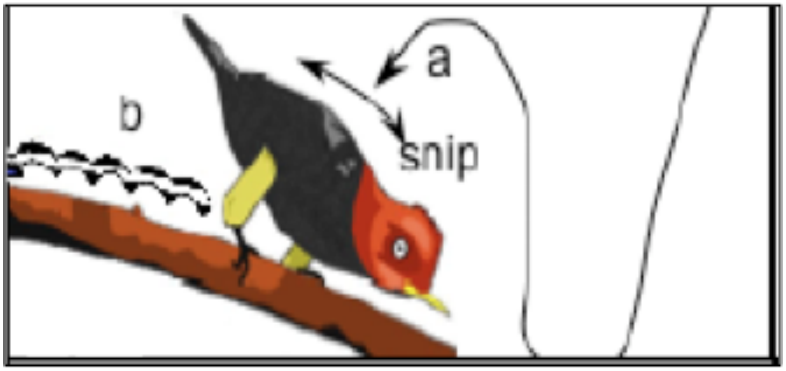

Figure 2. Depiction of *P. mentalis* courtship display. Bird swoops into the perch (a), making a wingsnip sound. Then the male "moonwalks," making small up-and-down hops very rapidly while moving backward (b).

Lance-tailed manakin (*C. lanceolata*) males are black with a red crown, blue upper wing coverts, and elongated central rectrices. These males' displays require cooperation of two individuals. The display occurs on a low horizontal liana 0.5 m to 2 m above the ground. One male flies and hovers approximately one quarter of a meter above the perch while another male slides under him across the vine. The hovering male then lands on the perch while the other male hops up to hover, and the male now on the perch slides under him. The males thus take turns in leap-frog fashion (Figure 3). Males also have a small mechanical sound repertoire (DuVal 2007).

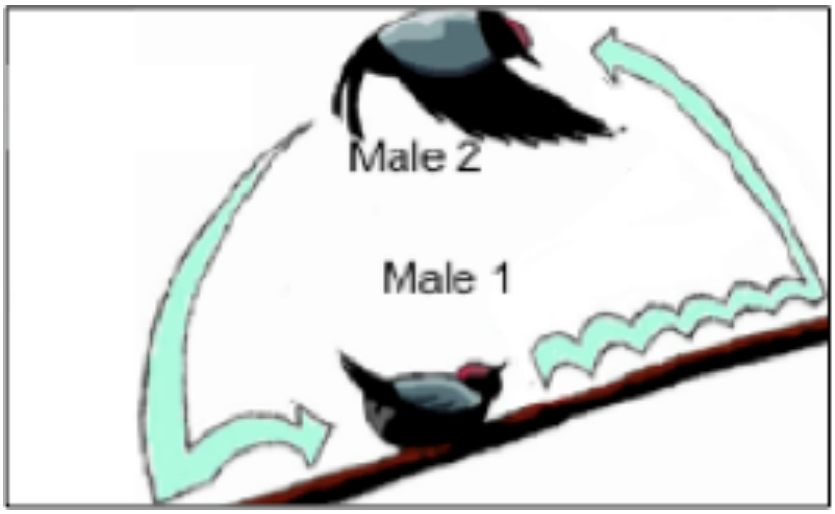

Figure 3. Depiction of *C. lanceolata* courtship display. The display always involves more than one male, and males alternately "leapfrog" over one another as shown.

Blue-crowned manakin (*L. coronata*) males are black with a blue crown. Their displays are the least complex of the species examined in this study. The display area consists of several display perches where a male perches and performs bowing and side-to-side jumping displays. Males also fly rapidly between perches and between small vertical saplings (Figure 4). No mechanical sounds are produced. Males chase each other using deep, exaggerated wing beats, a behavior which is considered to be a low level of male-male coordination (Skutch 1969; Duraes et al. 2007).

Figure 4. Depiction of *L. coronata* courtship display. Display consists mostly of simple flights between perches.

The ochre-bellied flycatcher (*M. oleagineus*) is a member of the tyrant flycatchers (Tyrannidae). Similar to the manakins, this species is lekking, frugivorous, and lives sympatrically with the manakins examined in this study. Male *M. oleagineus* also perform a simple courtship display, making this species a good non-manakin to examine. Males' displays involve a perched, crouching posture with exaggerated wing flicks. A male then proceeds to perform flight displays, which involve rapid flights between perches; slow butterfly-like flights between perches, similar to flights seen in *C. lanceolata* and *L. coronata*; and hovering several seconds above a perch (Westcott 1994).

iv. CEREBELLUM ANATOMY OVERVIEW

The Cb can be divided into the deep Cb nuclei and a surrounding cortex. The cortex consists of three layers: granular layer, PC layer, and molecular cell layer (Figure 5). The Cb nuclei in birds are homologous to those in humans and follow similar organizational principles: the CbL is more corticocerebellar while the CbM is more spinocerebellar (Arends & Zeigler 1991b; Wild & Williams 2000). The CbM projects to a number of regions in the brainstem and spinal cord: vestibular complex, reticular nuclei, plexus of Horsley portion of the parvicellular reticular formation, nucleus centralis medullae oblongatae, pars dorsalis, intermediate layer VII of the cervical spinal cord extending to cervical segment 8-

9, dorsal lamella of the inferior olive, locus coeruleus, dorsal subcoerulean nucleus, and motor trigeminal nucleus (Arends & Zeigler 1991b). The CbL sends mostly ascending fibers to midbrain and brainstem areas: red nucleus, nucleus of Cajal, midbrain central grey, prerubral fields, nucleus intercalatus thalami, ventrolateral thalamic nucleus, medial spiriform nucleus, nucleus principalis precommissuralis, nucleus of the basal optic root, nucleus geniculatus lateralis pars ventralis, dorsolateral thalamus, papilioform nucleus, medial pontine nucleus, gigantocellular and paramedian reticular nuclei, and inferior olive (Arends & Zeigler 1991b). These connections suggest that the CbL is involved in motor planning and cognitive aspects (Schwarz & Schwarz 1986), while the CbM is more involved in controlling postural muscles (Karten & Finger 1976; Wild 1992; Necker & Neumann 1997; Person et al. 2008). The cells of the Cb nuclei are either large glutamatergic projection neurons or small GABA-ergic interneurons. Further characterizations of these neurons using immunohistochemistry to identify the expression of several antigens within the nuclei has revealed a more complex differentiation of neurons within the Cb nuclei (Chung et al. 2009; Paxinos et al. 1999).

The cortical region of the Cb in birds is divided into ten distinct structures called folia (labeled I-X) and, if necessary, further divided anteroposteriorly into subfolia (ex. VIa, VIb; Figure 7). Mossy fiber inputs from the spinal cord, brain stem, reticular and pontine nuclei, and cerebral cortex to the Cb synapse with granule cells in the Cb cortex (Figure 6). The granule cell axons form excitatory parallel fibers in the superficial molecular layer and synapse with Purkinje cell dendrites, stellate cells, and basket cells. It has been proposed that the granular layer transforms the mossy fiber inputs to generate well-timed spike bursts to the molecular layer (D'Angelo & De Zeeuw 2009). Basket cells and stellate cells in

the molecular layer then form inhibitory synapses on Purkinje cell dendrites and soma. The PCs form a single-cell layer between the granular layer and the molecular layer and are the sole output cells of the cortex. They send inhibitory projections to the Cb nuclei. The Cb nuclei then send mostly glutamatergic excitatory projections to their targets, as well as some inhibitory projections to the inferior olive. In addition to mossy fibers, climbing fibers, another type of Cb input, arise from the inferior olive, which receives somatosensory, visual and cerebral cortical information. Climbing fibers from a particular set of olivary neurons have excitatory synapses on PCs as well as excitatory collaterals that synapse on the same Cb nuclei neurons that receive projections from those PCs. The nuclear cells then project back to the original olivary neurons. These loops are called olivocorticonuclear complexes or modules. The different components described in this paragraph play different roles in Cb processing, and I have measured several of these components to determine which aspects of Cb function relate to manakin display complexity.

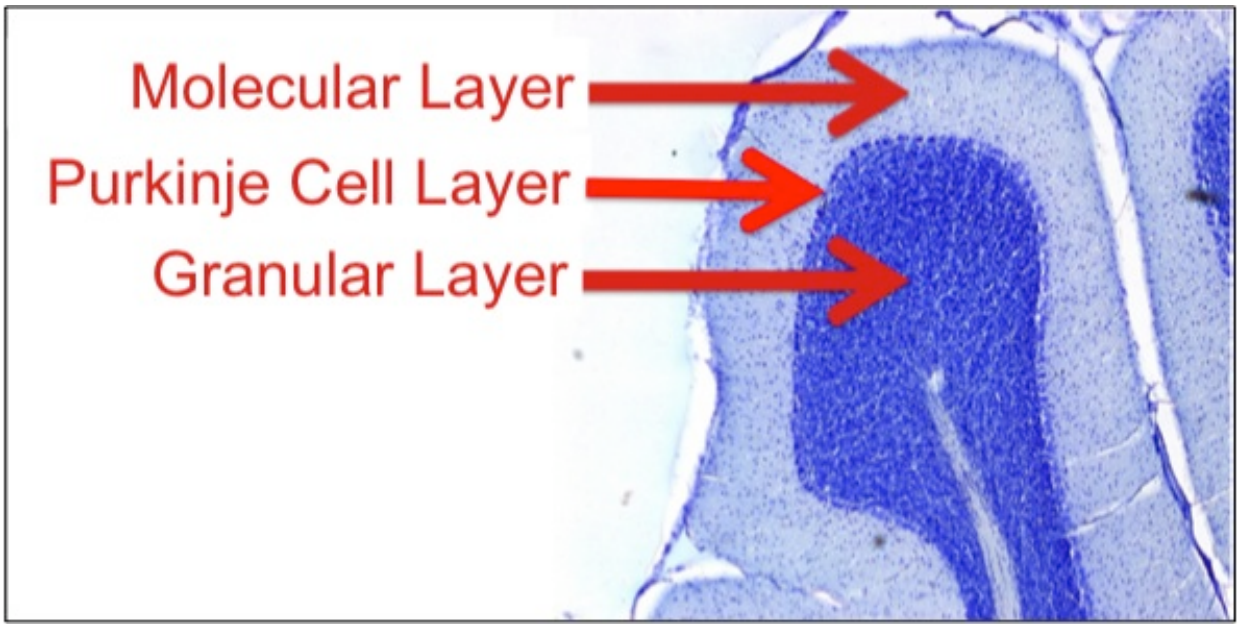

Figure 5. Cerebellar cortex. The molecular layer is the most superficial layer and consists mostly of the dendrites of PCs. The Purkinje cell (PC) layer is a single-celled layer of large PCs that are the sole output neurons of the Cb cortex. The granular layer consists of densely packed granule cells that relay mossy fiber inputs to the molecular layer.

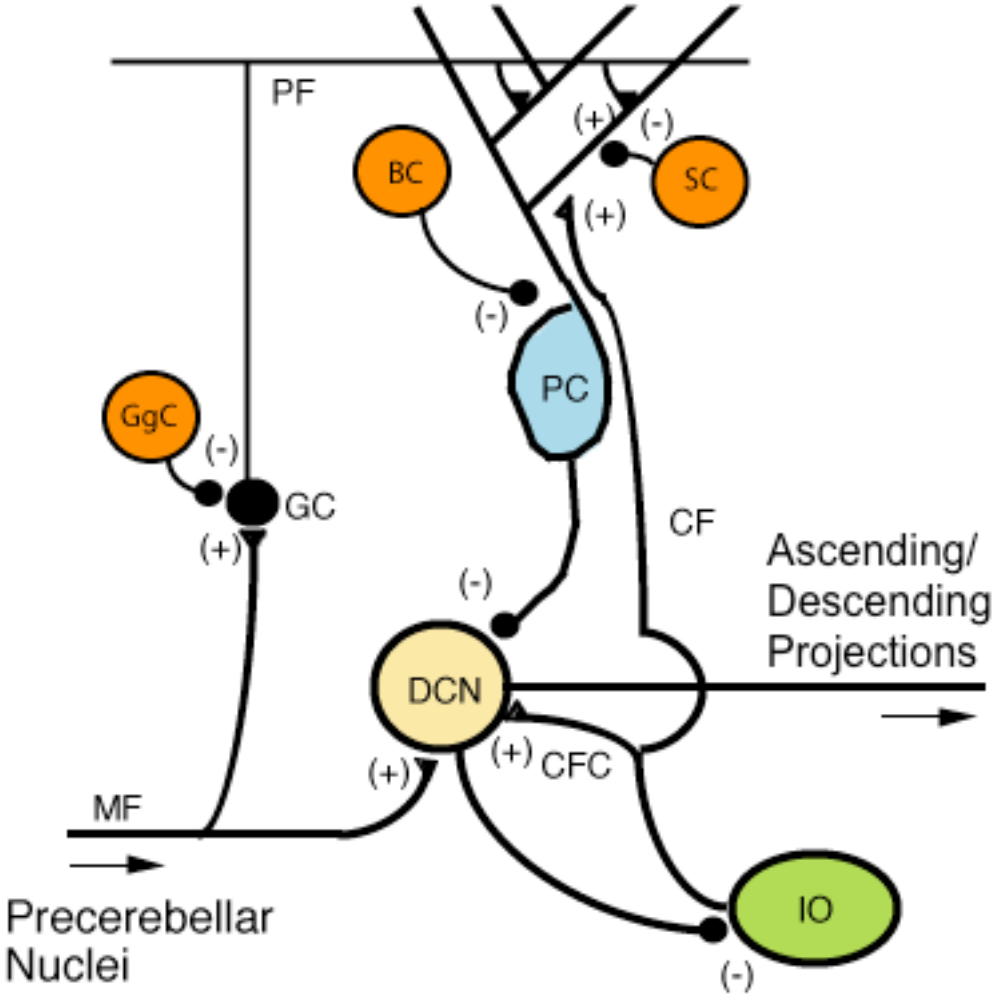

Figure 6. Cb circuitry. Excitatory mossy fiber (MF) inputs synapse on granule cells (GC), the axons of which form excitatory parallel fibers (PF) in the molecular layer. PCs are the sole output of the Cb cortex and send inhibitory projections to the cerebellar nuclei (DCN), which also receive excitatory inputs from MF collaterals. The DCN then project out of the Cb. Golgi cell (GgC) modify inputs to GCs, while basket cells (BC) and stellate cells (SC) modify inputs to PCs in the molecular layer. Olivocorticonuclear complexes consist of excitatory climbing fiber (CF) projections from the IO to the PC/molecular layer with collateral climbing fibers (CFC) to the DCN. The PCs receiving the CF then project to that very same part of the DCN receiving the CFCs, and then the DCN sends an inhibitory projection back to the original set of neurons in IO.

v. HISTORY OF RESEARCH INTO FUNCTIONAL ORGANIZATION OF THE CEREBELLUM

Initial investigations into the functional organization of the Cb were done in mammals. Because the Cb is a highly homologous structure, I describe in detail findings

regarding the mammalian Cb as these findings may also apply to the avian Cb. The idea that the Cb is somatotopically organized was denied by 19th century scientists (Luciani 1891), and although early reports provided evidence of potential functional organization (Sherrington 1897; Lowenthal & Horsley 1897), the scientific community overlooked them (Manni & Petrosini 2004). However, in 1904 two researchers working independently of one another published influential reports of functional localizations in the Cb (Bolk 1904; Pagano 1904). Bolk (1904) used careful phylogenetic comparisons in mammals of Cb anatomy to determine locations of functional areas, while Pagano (1904) utilized direct experimentation by injecting curare into different areas of the animal Cb and observing the effects. Both researchers simultaneously concluded that what are now referred to as lobules or folia I and II (Larsell 1947, 1948) are involved in limb coordination. In the 1940s electrophysiological techniques were employed to investigate afferents to the Cb, and these results shifted representations of the limbs to lobules III and IV, as well as completely reversed the map created by Bolk and instead suggested a body representation going roughly head-to-toe, posteroanteriorly within the Cb anterior lobe (Adrian 1943; Snider 1944) with more diffuse representations in the posterior lobe (Snider 1944). This shows that there may be multiple somatotopies, each detected by different methods, or there may be one somatotopy that neither method alone is sufficient to detect. Snider and Stowell (1944) also described visual and auditory inputs to lobules VI and VII. The Cb, however, is not so simple. Snider and Stowell's (1944) recordings were performed in anesthetized animals, and many of these results have not been replicated in awake animals (Manni & Petrosini 2004). Nevertheless, in recent studies in humans using imaging techniques such as positron emission tomography (PET) and functional magnetic resonance imagining

(fMRI), the existence of the two homunculi, one in the anterior and one in the posterior lobe have been confirmed (Manni & Petrosini 2004), but with considerable noise caused by other relevant features of Cb organization.

From anterograde and retrograde tracings, one concludes that the main efferent and afferent projections are organized in a band-like parasagittal topography. There also exist parasagittal divisions of the Cb into olivocorticonuclear complexes which consist of modules of distinct groups of inferior olivary neurons, climbing fibers, and deep cerebellar nuclei neurons (Figure 6; Garwicz 1992; Trott 1987; Trott & Armstrong 1987; Ekerot 1979). These in turn can be divided into microzones that consist of groups of climbing fibers, with the same receptive fields, that innervate small groups of Purkinje cells that project to specific deep cerebellar nuclei neurons (Trott 1987; Andersson 1978). Some of these microzones are somatotopically organized while others respond to different types or aspects of movement in rats (Manni & Petrosini 2004).

More recently it has been shown with molecular markers that Cb nuclei are compartmentally organized into at least twelve topological expression domains (Chung et al. 2009). Therefore, Cb morphology—including deep cerebellar nuclei (Van Kan 1993; Asanuma 1983) as well as cortex –may contain somatotopic body representations, and the functional topology of the Cb reflects more complex functional classifications. Further evidence of localization of complex functions is seen in fMRI studies in humans. Stoodley (2010) examined fMRI recordings during five different motor and cognitive tasks, such as finger tapping and mental rotation, and found that each task consistently activated distinct areas of the cortex that corresponded either to specific lobules or to functional zones, which could represent olivocorticonuclear modules. In addition, the Cb nuclei can be

divided into distinct regions based on connectivity with the Cb cortex (Sugihara & Shinoda 2007). Together, these findings suggest that functional connectivity of the Cb cortex and nuclei may be spatially partitioned. Given the homologous nature of the Cb in vertebrates, most of the features demonstrated in mammals and described in this section likely apply to the avian Cb.

vi. FUNCTIONAL ORGANIZATION OF THE AVIAN CEREBELLUM

Specific functions have been ascribed to specific morphology of the avian Cb, and the current study investigates this Cb morphology as it relates to manakin displays. As in mammals, the folia are grouped anatomically into the anterior lobe (I-V), posterior lobe (VI-IXcd) and vestibular cerebellum (IXcd-X), and specific folia are thought to be related to certain parts of the body or to have certain functions (Table 1). Folia I-III likely are involved in coordinating hindlimb muscles, as bird families with small hindlimb muscles and minimal behavioral use of the hindlimbs exhibit large reductions in these folia (Larsell 1967; Zusi & Bentz 1984; Cleere 1998; Iwaniuk et al. 2006b). In a recent, large comparative study, species classified as having strong hindlimbs have significantly larger anterior lobes and smaller posterior lobes than other species, and species classified as strong fliers have significantly smaller folia I-III and larger folia VI-VII (Iwaniuk et al. 2007). The larger VI-VII in strong flyers likely reflects increased visual demands during flight, as folia VII and the posterior part if VI respond strongly to visual stimulation in electrophysiological studies (Whitlock 1952; Gross 1970; Clarke 1974), and these folia appear enlarged specifically in raptors, which have good visual acuity (Larsell 1967). Folia VIII responds mostly to auditory stimuli in electrophysiological studies (Whitlock 1952; Gross 1970). Expression

patterns of the immediate early gene, ZENK, confirm some of these comparative findings. Expression in hopping finches and parrots and walking doves in the dark is localized to the anterior lobe, VI, and IXcd (Feenders et al. 2008). Warblers wing whirring in dim light exhibited similar ZENK distribution with additional expression in VII. Therefore, there is some consensus in the distribution of functions across the folia—e.g. vision is localized to VII and leg use is localized to the anterior lobe. The current study may provide additional support for this localization of function or help to refine these functional localizations. Largely consistent with the Feenders et al. (2008) findings, electrophysiology experiments show that folia II-VI and IX respond to somatosensory stimuli of the wings and legs (Schulte & Necker 1998). To summarize, there is consistent evidence that hindlimb function is associated with folia I, II, III, IV, V, VI, IX, and X; wing function with I, II, III, IV, V, VI, VII, IXcd, X; vision with VII; and audition with VIII. Overlapping somatotopies seen in the previous studies are likely due to measurement of different functions—e.g. complex motor and sensory aspects of hopping and wing whirring versus somatosensory stimulation in an anesthetized animal.

Table 1. Cb folia function summary based on comparative, electrophysiology, and ZENK studies described above. (1) Comparative: Larsell (1967), Zusi & Bentz (1984), Cleere (1998), Iwaniuk et al. (2006b & 2007); (2) Electrophysiology: Schulte & Necker (1998); (3) ZENK: Feenders et al. (2008); (4) Comparative: Iwaniuk et al. (2007); (5) Comparative and Electrophysiology: Larsell (1967), Whitlock (1952), Gross (1970), Clarke (1974); (6) Elecrophysiology: Whitlock (1952), Gross (1970); (7) Retrograde tracing: Pakan et al. (2008).

	Folium	Functions
AnteriorCb	I	hindlimbs[1], hopping[3], walking[3], wing-whirring[3]
	II	hindlimbs[1], somatosensory legs/wings[2], hopping[3], walking[3], wing-whirring[3]
	III	hindlimbs[1], somatosensory legs/wings[2], hopping[3], walking[3], wing-whirring[3]
	IV	somatosensory legs/wings[2], hopping[3], walking[3], wing-whirring[3]
	V	somatosensory legs/wings[2], hopping[3], walking[3], wing-whirring[3]
PosteriorCb	VI	flying[4], some vision[5], somatosensory legs/wings[2], hopping[3], walking[3], wing-whirring[3]
	VII	flying[4], vision[5], wing-whirring[3]
	VIII	audition[6]
	IXab	somatosensory legs/wings[2]
VestibuloCb	IXcd	somatosensory legs/wings[2], hopping[3], walking[3], wing-whirring[3], vestibular[7]
	X	somatosensory legs/wings[2], vestibular[7]

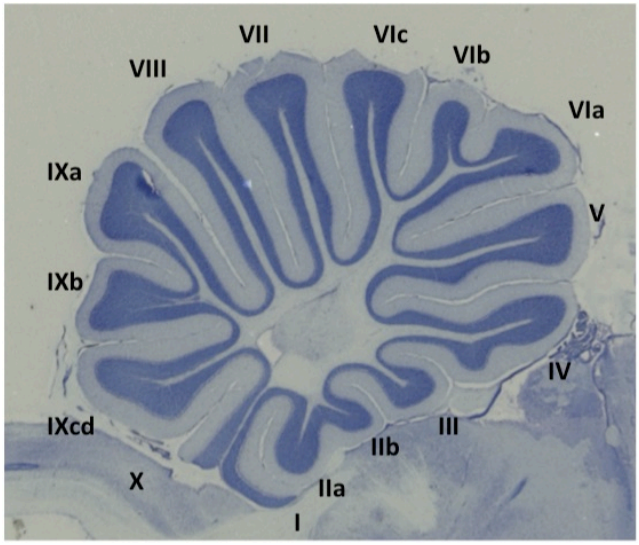

Figure 7. Nissl stained midsagittal section of golden-collared manakin Cb with folia and subfolia labeled. Anterior to the right.

Anterograde and retrograde tracings have been performed in pigeons to determine the corticonuclear and corticovestibular projections (Arends & Zeigler 1991a). Connectivity of the CbM and CbL does not differ with respect to the folia from which projections to CbM and CbL originate. Rather, as in mammals there appear to be longitudinal zones in which more medial PCs project to CbM while CbL receives projections from more lateral zones. These longitudinal zones may represent distinct functional areas that this study does not examine. The existence of longitudinal zones in birds is further demonstrated with zebrin II staining (Iwaniuk et al. 2009; Pakan et al. 2007). Recall that CbL projects to premotor and planning cerebrocortical regions while CbM projects to the brainstem and spinal cord. Therefore, by examining folial morphology (rostrocaudal) as well as CbM and CbL (longitudinal zones), this study has the potential to determine whether rostrocaudal or longitudinal functional organization is more important in manakin displays. Furthermore, since the CbM has mostly descending projections while the CbL has mostly ascending projections, this study may differentiate contributions from Cb motor loops versus those that are more pre-motor/cognitive, respectively.

No comparative studies or studies examining behavioral complexity directly demonstrate that features of Cb morphology measured in this study might relate to display complexity in manakins. However, many examples show that specific changes in Cb morphology can be associated with variation in behavior.

vii. BEHAVIORAL CORRELATES OF CEREBELLUM MORPHOLOGY

I described above that total Cb volume is correlated with bower complexity, but the following examples demonstrate that differences in specific aspects of Cb morphology can be associated with differences in behavior.

In humans, several disorders heavily affecting cognition, such as fragile X syndrome and attention deficit hyperactivity disorder, are associated with a decrease in the size of the posterior Cb (Steinlin 2008). Down syndrome, which is the most common cause for mental retardation (Hook 1981), is associated with a disproportionately greater reduction in cerebellar volume than other brain regions (Aylward et al. 1997). In the Down syndrome mouse model, Ts65Dn, a reduction in volume in the granular and molecular layers is observed but no impairment of motor function, suggesting that these layers may be more associated with cognitive behaviors (Moran et al. 2000).

PC deficits have also been shown specifically to affect behavior. In mutant mice strains in which PCs never develop or degenerate after birth—Lurcher or Shaker strains, respectively—mice develop a marked ataxia, indicating that these cells in particular are necessary for Cb motor function and that a decrease in PC number effects motor ability in an individual (D'Angelo 2009; Wolf et al. 1996). In humans cerebellar degeneration in alcoholics also is associated with ataxia, mainly of the lower limbs, and appears to be the result of a decrease in PC size (Andersen 2004).

The volumes of the Cb nuclei in several anthropoid species have been compared with respect to differing locomotor types and spatial habitats. In species of most locomotor types, CbL is relatively larger than CbM. However, arboreal quadrupeds, whose locomotor functions involve forelimb and hindlimb coordination in a 3-dimensional environment,

have Cb nuclei which are each similar in size to one another (Matano & Hirasaki 1997). Additionally, the authors of that study found that the enlargement of CbL versus CbM in humans is much greater than in other anthropoids and propose that the larger CbL, which is more corticocerebellar, in humans reflects their complex, voluntary finger movements and may even be an evolutionary prerequisite to language.

Given that these features of the Cb are capable of associating with behavioral variability, I examined whether Cb morphological features relate to the evolution of courtship behaviors in manakins. These courtship behaviors require complex acrobatic movements and likely require a great amount of Cb processing. By comparing manakin species with displays that vary in complexity, I sought to determine if specific Cb features are enlarged, presumably to allow for greater capabilities for Cb processing, in species with more complex displays. I hypothesized that Cb volume, PC size and density, and CbM and CbL volume and cell density would be most likely to increase with increasing display complexity because Cb volume represents total Cb processing capacity and the PCs and Cb nuclei are major convergence points for information within the Cb.

II. METHODS

i. SCORING DISPLAYS

In order to objectively quantify the display complexities of each species, published reports describing unique and shared display elements between each species were utilized. Scores were determined from rigorous descriptions and summaries by Prum (1990), as well as additional descriptions of social behavior and mechanical sounds (Chapman 1935; Prum 1994; Prum 1998; DuVal 2007; Bostwick & Prum 2003; Duraes et al. 2007). The information utilized in scoring the displays are 1) Number of discrete display elements performed and type of display site (Table 2, "Display Characters"), 2) Level of social interaction between displaying males (Table 2, "Cooperation"), and 3) Presence, number and type of mechanical sounds produced (Table 2, "Mechanical Score"). The scores for each criterion were added together to create the overall Display Complexity score (Table 2).

Table 2. Display complexity score breakdown. Display Complexity equals the sum of Mechanical Score, Cooperation, and Display Character columns.

Species	Display Complexity	Mechanical Score	Cooperation	Display Characters
Manacus vitellinus	28	10	1	17
Chiroxiphia lanceolata	22	7	2	13
Pipra mentalis	18	8	0	10
Lepidothrix coronata	11	0	1	10
Mionectes oleagineus	3	0	0	3

The number of Display Characters refers to the total number of discrete display elements described in the literature. These elements include such behaviors as frenzied-flutter flights, to-and-fro hops, butterfly chases, and swoop flights (Prum 1990). The type of display perch was also included in Display Characters. A species received one point for using only one or a couple of horizontal perches, two points for using a fallen log (a very specific display perch), three points for using a loose court of several perches, and four points for actually clearing an arena and manipulating the environment to produce the court. The Mechanical Score adds information regarding the presence of mechanical sounds in the display (1 point), the number of display elements that include mechanical sounds, the number of sounds per element, and whether the species is capable of producing mechanical sounds in flight (2 points), only perched (1 point), or both (3 points). Cooperative displays involve two or more individuals who behave together. One point was given for the presence of coordinated display elements that also may be performed solo, and 2 points was given if there were display elements in the species' repertoire that may only be performed cooperatively.

ii. OBTAINING SPECIMENS

In June-August of 2008 and 2009, I collected a total of 15 adult male manakin specimens and two male flycatchers in Panama in the eastern Canal Zone near the town of Gamboa. This time period is within the breeding seasons for these species, but at the very early or very late end for some species, so the gonads were examined to determine presence of active spermatozoa using standard hematoxylin and eosin stain. Presence of spermatozoa confirms that the sampled individuals were in breeding condition. The

breeding specimens included three *Manacus vitellinus*, four *Pipra mentalis*, three *Chiroxiphia lanceolata*, three *Lepidothrix coronata* and two *Mionectes oleagineus*. All necessary permits were obtained from USDA, IACUC, and Panamanian authorities, Autoridad Nacional del Ambiente and Autoridad del Canal de Panama.

Mist nets were set up daily from 0600 to around 1300 and sometimes again from 1400 to 1700. Nets were checked every thirty minutes. Adult male manakins were identified by plumage. Birds were kept in a cloth bird bag for transport back to the laboratory for processing. *Mionectes oleagineus* is not sexually dimorphic in plumage, so specimens were sexed in the laboratory by examination of the gonads.

iii. TISSUE PREPARATION

Each specimen was transported to the field laboratory in Gamboa, usually within an hour of removal from the mist nets. They were then exposed to an overdose of isoflurane anesthetic. A peristaltic pump was used to perform a transcardial perfusion of the bird. The outflow needle of the pump was placed in the left ventricle of the heart, and the jugular vein was severed to allow fluids to flow out after traveling through the body. Approximately 30 ml 0.1M phosphate-buffered saline (PBS) solution was slowly (appx. 3ml/min) pumped through the bird followed by 40 ml 10% neutral-buffered formalin (NBF). The brain was then dissected out and placed in NBF for 24 hours of post-fixation before being transferred to 20% (w/v) sucrose in PBS for cryoprotection. After the brain sank (appx. 24 hours), indicating that the sucrose had permeated the tissue, it was solidified in a gel block of 8% (w/v) gelatin and 16% (w/v) sucrose in RO-H_20. The gel block was then placed in NBF for 24 hours to harden it and then transferred to 30% (w/v)

sucrose in PBS until it sank. Finally, the gel block was frozen and stored on dry ice until transferred to -80 °C at the University of Mississippi. The bodies, including gonads, were stored in formalin and kept at 4 °C.

For one specimen of each species, after the brain was dissected out and postfixed in NBF for 24 hours but before being cryoprotected, the brain was cut midsagittally using a razor blade. For one of the halves, the CB was then separated from the rest of the brain, and photographs were taken of the medial, lateral, and dorsal views for record of the orientation of the CB in relation the rest of the brain and to assist in defining folia. This tissue was otherwise treated as described above for the intact brains.

In the lab at the University of Mississippi, each whole brain was sectioned sagittally on a cryostat into 3 series at a thickness of 30 μm. One series of sections—i.e. every third section—was placed directly onto gelatinized slides and allowed to air-dry. The slides were then Nissl-stained with cresyl violet to define cells and nuclei. The second and third series were placed in cryoprotectant solution (Watson et al. 1984) and stored at -20°C to be used later for immunohistochemistry or other procedures.

iv. DATA COLLECTION

A. Confirmation of Breeding Condition

It was important that all individuals were in breeding condition when caught because seasonal fluctuation in brain region size has been shown to occur in birds (Brenowitz 1997). To confirm that all individuals were indeed in breeding condition, the testes were examined for spermatozoa production using hematoxylin and eosin stain. In breeding birds, the spermatozoa are clearly visible entering the seminiferous tubule

(Figure 8). A testis was dissected out of the body, then cryoprotected in 30% sucrose (w/v) in PBS until it sank. The testis was placed in a gelatin block (w/v), allowed to solidify, placed in NBF overnight, then cryoprotected in 30% sucrose (w/v) until it sank. Each testis was sectioned as thinly as possible (5-20 μm) without damaging tissue, and sections were placed on a gelatinized slide and allowed to dry. Sections on the slides were then stained with hematoxylin and eosin. Testes for *M. oleagineus* specimens were need by another lab for other purposes and not examined for spermatozoa, but the individuals were caught during their reported breeding seasons (Westcott 1994).

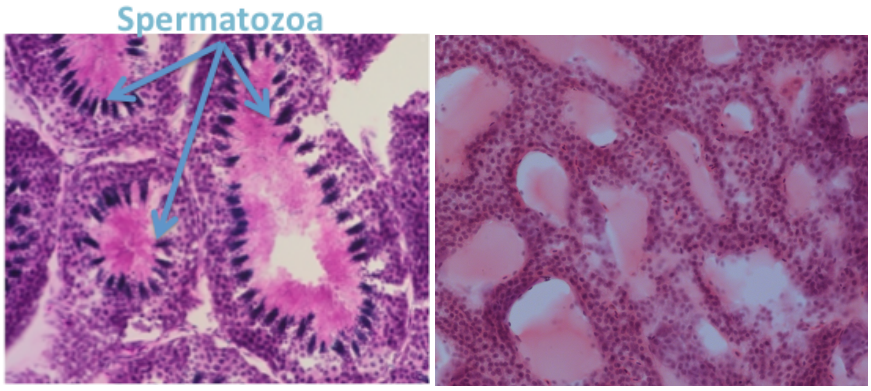

Figure 8. Left) Purple spermatozoa clearly lining the seminiferous tubules in testis of breeding bird. Right) No spermatozoa visible in non-breeding individual. Only manakin individuals producing spermatozoa were included in the study.

B. Whole brain, Cb, molecular layer, granular layer, and white matter volume measurements

Images of every 3rd section on the slides (ie. every 270 μm) were taken using a Zeiss Stemi 2000-CS dissecting microscope and Zeiss Axiocam HRc digital camera. Image J software from NIH was used to measure areas on each section, and estimates for whole brain volume, whole CB volume, molecular layer volume, granular layer volume, and Cb white matter volume for each specimen were determined using the Cavalieri estimator formula: estimated volume = (sum of cross-sectional areas) x (thickness of each section) x

(# sections between measured sections) (e.g. Rosen & Harry 1990). Hence, the sum of areas measured in cm^2 on each section was multiplied by 0.027 cm, the distance between slices, to give the volume estimate. White matter volume was determined by measuring the volume of the boundary of the white matter and granular layer, then subtracting the volume of the Cb nuclei. Granular layer volume was determined by measuring the volume within the granular layer and molecular layer, then subtracting the volume traced at the white matter/granular layer boundary (see Figure 5 in Introduction). Molecular layer volume was determined by subtracting the volume traced at the molecular/granular layer from total Cb volume.

C. Purkinje cell size and density

Using a Zeiss Imager.M1 microscope with Axiocam HRc camera and Axiovision image capture and analysis software, a random sampling scheme was employed to measure the size and density of Purkinje cells, the sole efferent source of the cerebellar cortex. The Purkinje cell layer is located at the boundary of the molecular and granular layers and is a single cell in thickness (Figure 9). Therefore, in tissue sections the linear density was measured. Measurements were done in the midsagittal section at 1000X magnification (Figure 9c), and the maximum cross-sectional area of an intact PC was measured. In order to prevent PC-profile-area underestimates, PC area was only measured if the cell was intact and a nucleolus was visible (Tran et al. 1998). Only a visible nucleolus was required to count a cell for density measurements. Each folium was measured from anterior to posterior. The first field-of-view (FOV) measured for each folium was decided by randomly obtaining a number between one and three. Then every third FOV was measured as one

moves along the PC layer while maximizing the layer length at each FOV. The leading edge of the PC layer in each FOV was considered forbidden and partial cells on that edge were not counted in order to prevent overestimation of cell number (Figure 9). PC density was measured by dividing the total number of cells by the total length measured in each FOV.

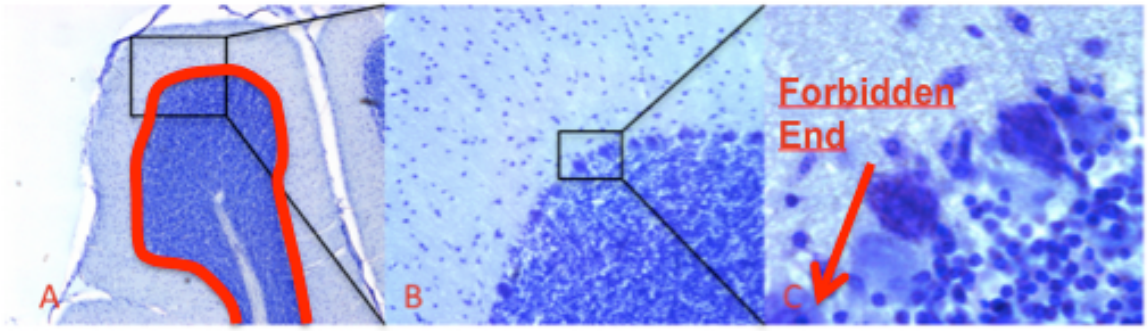

Figure 9. Views of the curving PC layer of the Cb. A) 50X magnification with PC layer shown by red line. B) 400X magnification, PCs visible. C) 1000X magnification for measuring PC cell size. Leading forbidden end of PC layer shown. Partial cell visible but not counted.

D. Cb nuclei volumes

The volumes of CbM and CbL were also calculated using the Cavalieri estimator formula. Area measurements, in cm^2, of CbM and CbL were made on each 30 µm section, which is separated by a gap of 60 µm. Therefore, the sum of areas was multiplied by 0.009 cm to obtain each volume estimate. Area measurements were made at 50X magnification using the same equipment as with PC measurements. The CbL was defined as the collection of large neurons located superior to the lateral cerebellar peduncles, and the CbM was defined as the collection of large neurons superior and medial to the cerebellar peduncles, with reference to zebra finch and pigeon atlases (Figure 10; Karten 1967; Nixdorf-Bergweiler & Bischof 2007).

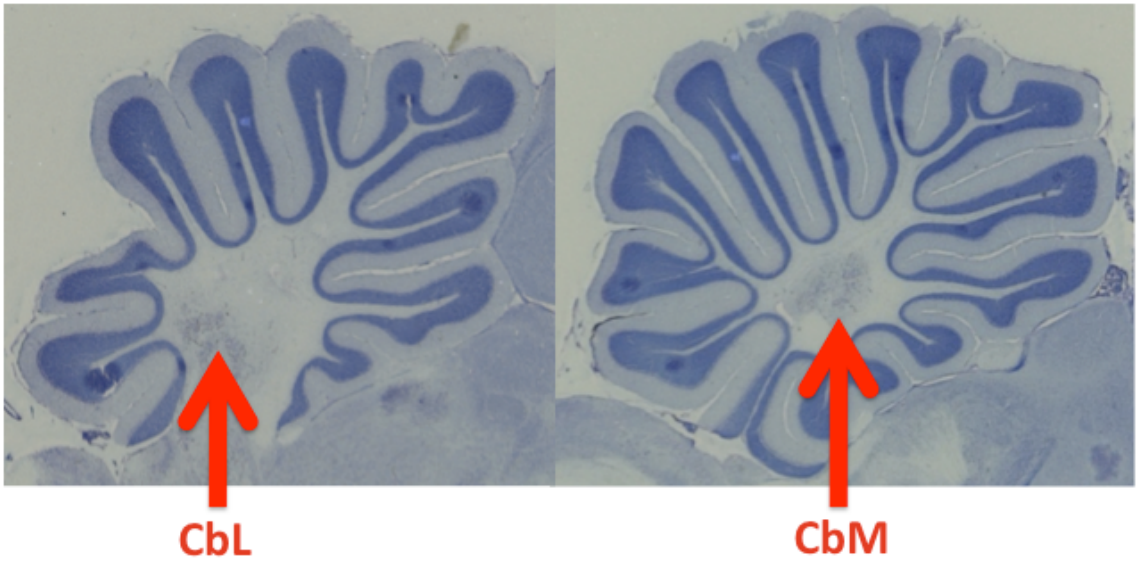

Figure 10. Sagittal sections of the cerebellum. Left frame) CbL is located in lateral sections superior to the cerebellar peduncles where white matter enters and exits the Cb. Right frame) CbM is located in sections medial to the cerebellar peduncles.

E. Cb nuclei cell densities

Cell density was determined at 1000X magnification using the same Zeiss equipment as for PC and Cb nuclei measurements. First, a grid was created at 50X magnification such that each square was the size of a FOV at 1000X. For CbM, a random number between one and four was generated, then that number of squares was counted down from the top left square. Starting with the next square down, in every fourth square for which the top right corner lay within the region, the number of cells was counted at 1000X. For CbL, cells were counted in all squares because the region is smaller than the CbM. This sampling scheme resulted in an acceptable coefficient of error (Schmitz & Hof 2000), less than 0.1, for each species data point (Gokcimen et al. 2007). The microscope focus was adjusted in-and-out to determine depth boundaries, and only cells for which an in-focus nucleolus, full or partial, was visible were counted, except cells crossing the bottom or left edges, which were considered forbidden. These measurements were

performed on every 4th section through the cerebellum, and the first section was chosen by obtaining a random number between one and four. Then the volume of each FOV was calculated by multiplying section thickness, 0.003 cm, by the area of the square, 0.000059965 cm^2. The total number of cells from each FOV measured for a specimen was added together, then divided by the total number of FOVs. This density was divided by the volume of a FOV to give density in number-of-cells/cm^3.

F. Anterior, posterior, and vestibular Cb size

Measurements were done in Image J using the same sections as with Cb volume measurements. The length of the PC layer in the midsagittal section was measured as a proxy for anterior Cb size (folia I-V), posterior Cb size (VI-IXcd), and vestibular Cb size (IXcd-X). The length of the PC layer in the midsagittal section is known to correlate well with Cb volume and has been used to measure folia size in other studies (Iwaniuk et al. 2007).

v. DATA ANALYSIS

Analyses were performed on both phylogenetically corrected species contrast means and non-corrected means. I used both corrected and non-corrected species means because the phylogenetic correction reduces n from 5 to 4, reducing statistical power, and hence may distort true relationships rather than reveal them.

Prior to analyses, all morphology data was ln-transformed to improve fit to normality. Then each variable was corrected for any allometric effects. Allometric effects involve the scaling up of organ structure sizes in larger animals (e.g. West et al. 1997). For

example, the size of the Cb in bowerbirds is correlated with bird weight (Day et al. 2005). Therefore, if allometry exists in these manakin specimens for the Cb measurements, they need to be corrected to standardize comparisons of specific brain morphology. To determine if allometric corrections were necessary, I performed stepwise linear regressions with each morphological variable as responses and candidate covariates (Cb volume, Brain minus Cb volume, Brain Weight) as predictors to assess the predictive value of the potential covariates. If there was a significant covariate for the Cb morphology variable, this was used as a covariate to adjust the value of this measurement.

Next, general linear models (GLM) were run with each morphological variable as the response, Species as a fixed factor, and any covariates, as determined from the stepwise regression. If there was no significant interaction between Species and the covariates, the interaction term was removed from the model. Marginal means (species means adjusted for covariates) from the GLM for each species were then used for comparison with Display Complexity.

To correct for species relatedness, phylogenetically independent contrasts were created for marginal species means for Cb morphology, along with the Display Complexity, using the computer software module PDAP (Midford et al. 2005) run within the software Mesquite (Maddison & Maddison 2006). This is necessary because the species in the study are relatively closely related and, hence, may not be considered independent data points. Independent contrasts are generated between each node in the phylogeny, also taking into account the distance between those nodes. The topology of relationships used to generate the contrasts was created using a molecular tree created by McKay et al. (2010) based on the mitochondrial ND2 and COI loci and nuclear MUSK intron 3 (Figure 11). Because this

phylogeny did not include the ochre-bellied flycatcher (*M. oleaginous*), branch lengths between each node were set equal to one. Setting each branch length to one is the most unbiased method of assigning values to unknown branch lengths. Display complexity scores and the independent contrasts from each Cb morphological variable were then analyzed using simple regressions forced through the origin as required for independent contrast correlations. This analysis tells one if the brain region in question and display complexity evolved together.

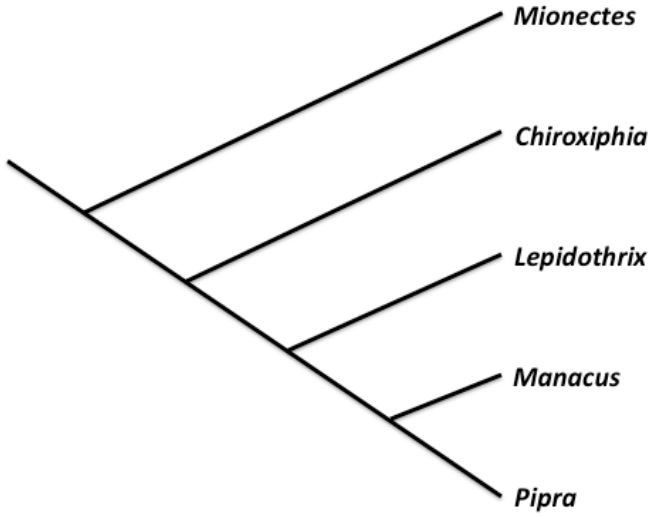

Figure 11. Phylogenetic tree of manakin species with flycatcher (Mionectes) outgroup used to create independent contrasts. Topology from McKay et al. (2010).

Next, simple regressions of each Cb morphological variable versus Display Score were performed. I used these regressions to reduce the number of variables that would be included in a more complex model. This was necessary because there were more variables than species. Only Cb morphology variables that were nearly significant ($p \leq 0.10$) for the non-corrected marginal mean analyses or the corrected contrast analyses were further

tested in a stepwise multiple regression. Two separate stepwise regressions were performed, one for phylogenetically corrected data and one for non-corrected data.

Historically, Cb folia have been described as species-specific (Larsell 1967), using only single individuals as representatives (Iwaniuk et al. 2007), but this study utilizes multiple individuals of each species. Therefore, foliation patterns were examined across individuals within each species to determine if this assumption was valid. Furthermore, since the degree of foliation has been shown to relate to the size of the Cb across orders of birds, a cerebellar foliation index (CFI; Iwaniuk et al. 2006a) for each specimen was generated to represent the degree of foliation, and these indices were regressed against Cb Volume to determine if this relationship holds within more closely related species. The CFI was calculated in the midsagittal section as the length of the PC layer divided by the cerebellar envelope as in Iwaniuk et al. (2006a; Figure 12).

Figure 12. Envelope drawn around tips of folia at the PC layer. The CFI was calculated as the total length of the PC layer (see Figures 5 & 10) in the midsagittal section divided by the envelope: CFI = PC Layer / Envelope.

III. RESULTS

i. CB FOLIATION

Upon examination of subfolia in all specimens, only folia II, IV, VI, and IX ever split into subfolia. Within each of the five species examined in this thesis, there is variation in the number of subfolia between individuals within a species: *M. vitellinus* (n=4) in folia II, IV and VI (Figure 13); *P. mentalis* (n=3) in folium VI (Figure 14); *C. lanceolata* (n=3) in folia IV and VI (Figure 15); *M. oleagineus* (n=3) in folia II and VI (Figure 16); and *L. coronata* (n=4) in folium VI (Figure 17). One individual of *L. coronata* actually has an entire extra folium between II and IV.

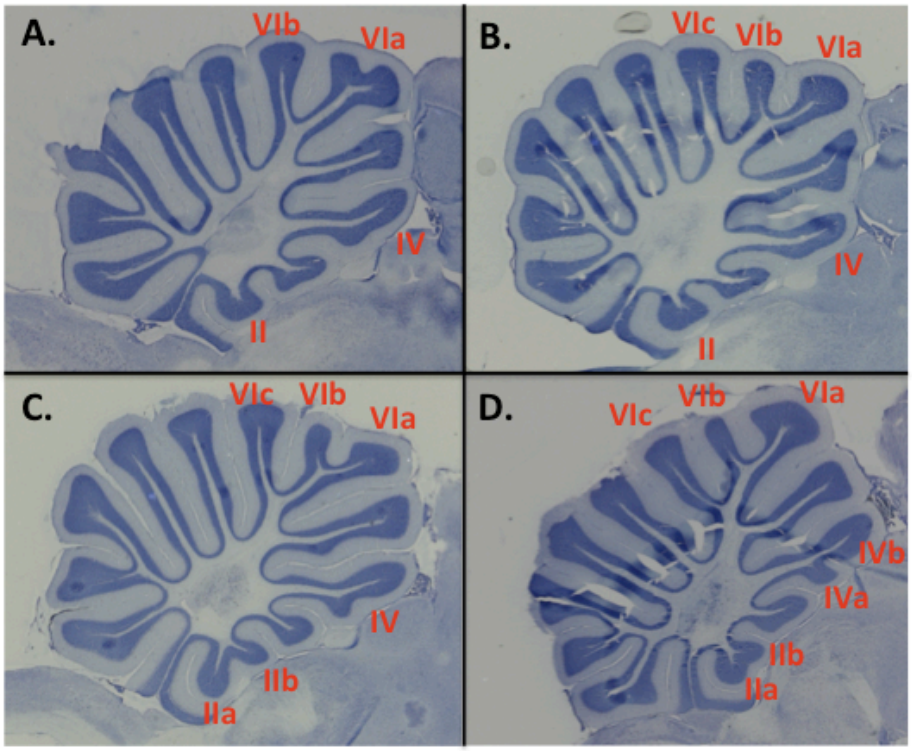

Figure 13. Golden-collared manakin (*M. vitellinus*) subfoliation differences across four specimens. Folium II: (A) and (B) have single folium while (C) and (D) have two subfolia. Folium IV: (A), (B), and (C) have one folium while (D) has two subfolia. Folium VI: (A) has two subfolia while (B), (C), and (D) have three subfolia.

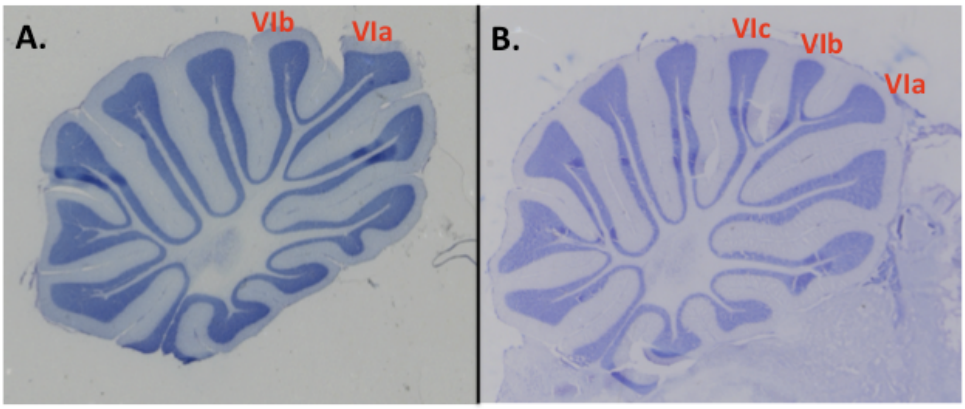

Figure 14. Red-capped manakin (*P. mentalis*) subfoliation differences between two specimens. Folium VI: (A) has two subfolia while (B) has three subfolia.

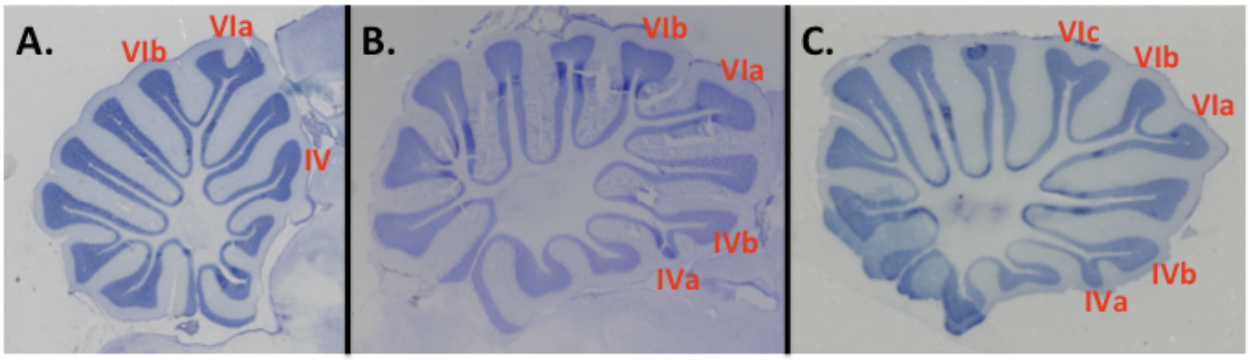

Figure 15. Lance-tailed manakin (*C. lanceolata*) differences in subfoliation across three specimens. Folium IV: (A) has one folium while (B) and (C) have two subfolia. Folium VI: (A) and (B) have two subfolia while (C) has three subfolia.

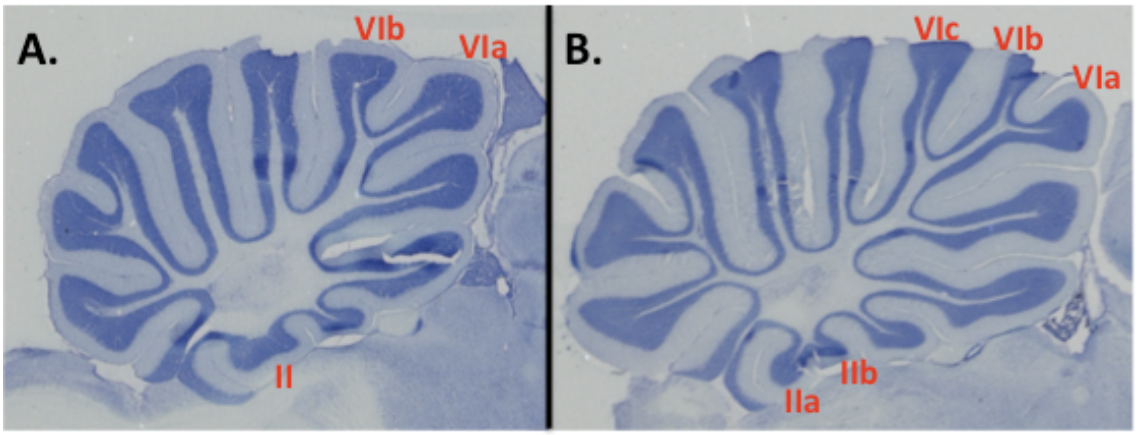

Figure 16. Ochre-bellied flycatcher (*M. oleagineus*) differences in subfoliation between two specimens. Folium II: (A) has one folium, though it appears widened, while (B) has two subfolia. Folium VI: (A) has two subfolia while (B) has three subfolia.

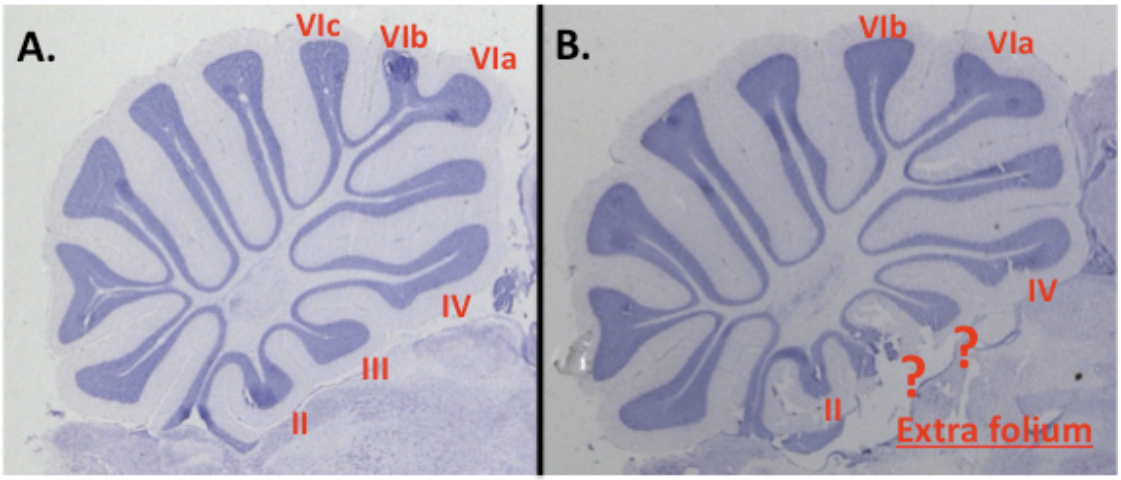

Figure 17. Blue-crowned manakin (*L. coronata*). Folium VI: (A) has three subfolia while (B) has two subfolia. In (B), between folia II and IV there is an entire extra folium that does not appear to be a subfolia of either II, III or IV.

In a regression of CFI versus Cb Volume in all individuals, including two additional manakins whose testes were in non-breeding condition, a positive relationship was detected ($F_{(1,16)} = 6.992$, $p = 0.018$, $r^2 = 0.32$; Figure 18). This suggests that the amount of foliation can be partially explained by the size of the Cb. Because of the unexpected variation in foliation patterns within species, only measurements of anterior, posterior and vestibular Cb were done rather than measurements of individual folia.

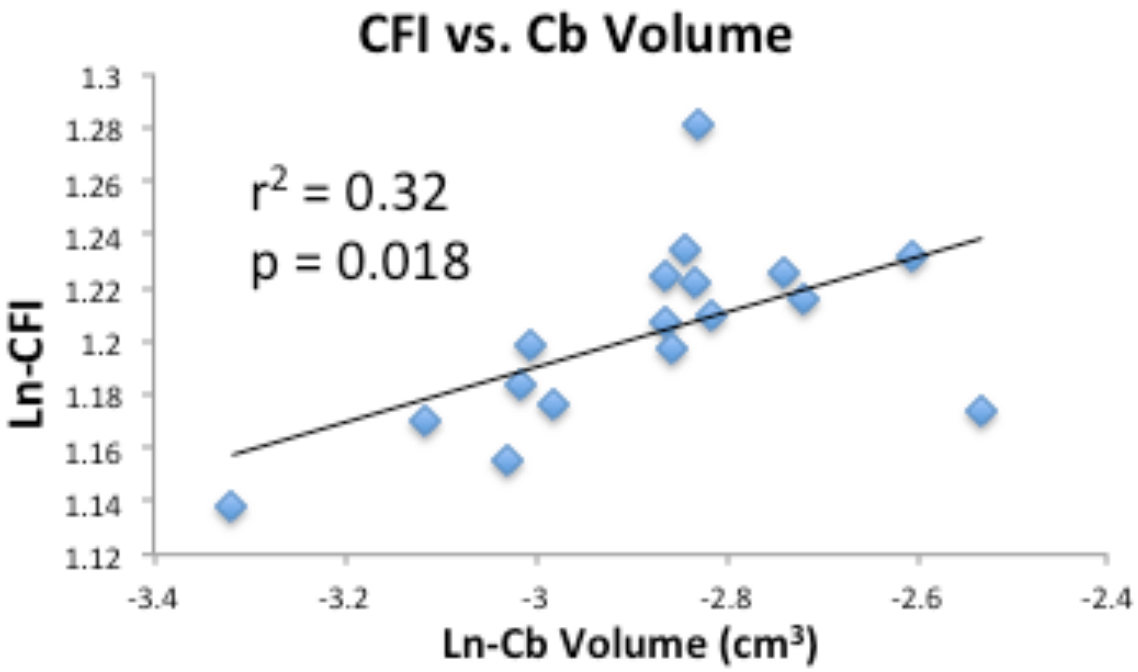

Figure 18. Regression of Ln-CFI versus Ln-Cb Volume. There was a significant positive relationship, suggesting that in these specimens having a greater degree of foliation in the Cb is partially the result of having a larger Cb.

ii. CB MORPHOLOGY AND DISPLAY COMPLEXITY

Stepwise multiple regressions were performed to determine which potential covariates contributed to allometric effects. Potential covariates tested for Cb Volume

included Brain minus Cb Volume and Brain Weight. For all other variables, potential covariates included Cb Volume, Brain minus Cb Volume, and Brain Weight. Table 3 lists each morphology variable and the significance of covariates. Where no covariate was significant, a correction factor is not necessary in the GLM.

Table 3. Results of stepwise multiple regressions for each Cb morphology variable and its potential covariates. Cb morphology variables were later corrected for allometric scaling with significant covariates. $\alpha = 0.05$. Dash ("-") indicates no significant covariate.

Cb Morphology Variable	Covariate	R^2_{adj}	p
Cb Volume	Brain minus Cb Volume	0.640	<0.001
CbM Volume	Cb Volume	0.240	0.037
CbL Volume	Brain Weight	0.265	0.029
CbM+CbL Volume	Brain Weight	0.238	0.038
CbM # Cells	-	-	-
CbL # Cells	-	-	-
CbM+CbL # Cells	-	-	-
CbM Cell Density	Brain Weight	0.338	0.014
	Cb Volume	0.504	0.006
CbL Cell Density	-	-	-
CbM+CbL Cell Density	-	-	-
Granular Layer Volume	Cb Volume	0.844	<0.001
White Matter Volume	Brain minus Cb Volume	0.730	<0.001
Molecular Layer Volume	Cb Volume	0.765	<0.001
PC Layer Length	Brain minus Cb Volume	0.594	<0.001
Anterior Cb Size	Cb Volume	0.865	<0.001
Posterior Cb Size	Cb Volume	0.489	0.002
Vestibular Cb Size	Cb Volume	0.797	<0.001
PC Size	Brain Weight	0.430	0.005
	Brain minus Cb Volume	0.571	0.002
PC Density	-	-	-
PC #	Cb Volume	0.545	0.001

The GLMs were run with each morphological variable as the response, Species as a fixed factor, and any appropriate variables as covariates as determined from the previous stepwise regressions (Table 3). There were no significant interactions detected between Species and covariates for any of the variables-of-interest. Therefore, the GLMs were run

again with the interaction term removed, and the marginal means for each species were obtained for use in comparisons with Display Complexity. If no covariates existed then species means were calculated without using GLMs. In the individual linear regressions of Cb morphological variables versus Display Complexity, I used a cutoff of $p < 0.1$ rather than 0.05 to decide which Cb variables to include in a multiple regression because the sample size was somewhat low, reducing statistical power. Individual regression results are summarized in Table 4. Given the potential association of Vestibular Cb Size with display, additional measurements in the vestibular Cb—PC size, density and number—were included to determine if there might be further associations in the vestibular Cb.

Table 4. Results from linear regressions of each non-phylogenetically corrected Cb morphology variable vs. Display Complexity. The sign of the relationship is given for variables for which $p < 0.1$, highlighted in blue. These variables were then tested in a stepwise regression.

Cb Morphology Variable	r^2	p	slope
CbL Volume	0.05	0.706	
CbM Volume	0.70	0.078	pos.
CbL+CbM Volume	0.59	0.129	
CbL Cell Density	0.20	0.447	
CbM Cell Density	0.58	0.133	
CbL+CbM Cell Density	0.38	0.265	
CbL # Cells	0.26	0.383	
CbM # Cells	0.00	0.963	
CbL+CbM # Cells	0.09	0.620	
Cb Volume	0.31	0.329	
White Matter	0.72	0.071	pos.
Molecular Layer	0.59	0.127	
Granule Layer	0.14	0.535	
PC Layer Length	0.27	0.368	
Anterior Cb Size	0.11	0.593	
Posterior Cb Size	0.14	0.531	
Vestibular Cb Size	0.78	0.046	neg.
PC Size, all folia	0.72	0.068	neg.
PC Density, all folia	0.12	0.571	
PC #, all folia	0.00	0.935	
Vestibular Cb PC Size	0.04	0.764	
Vestibular Cb PC Density	0.08	0.646	
Vestibular Cb PC #	0.18	0.478	

Variables for which $p < 0.1$—CbM Volume, White Matter Volume, Vestibular Cb, and PC Size—were then included in a stepwise multiple regression with entry probability of F set at 0.05 and removal probability of F set at 0.1. The resulting model included both Vestibular Cb and CbM Volume ($F_{(1,4)} = 337.3$, $R^2_{adj}=0.994$, $p=0.003$). Vestibular Cb was negatively related to Display Complexity while CbM Volume was positively related to Display Complexity. The collinearity tolerance for Vestibular Cb and CbM Volume was 0.76 indicating that these variables are independent of one another in the model. Figure 19

depicts the results from the individual linear regressions of Vestibular Cb Size vs. Display Complexity and CbM Volume vs. Display Complexity.

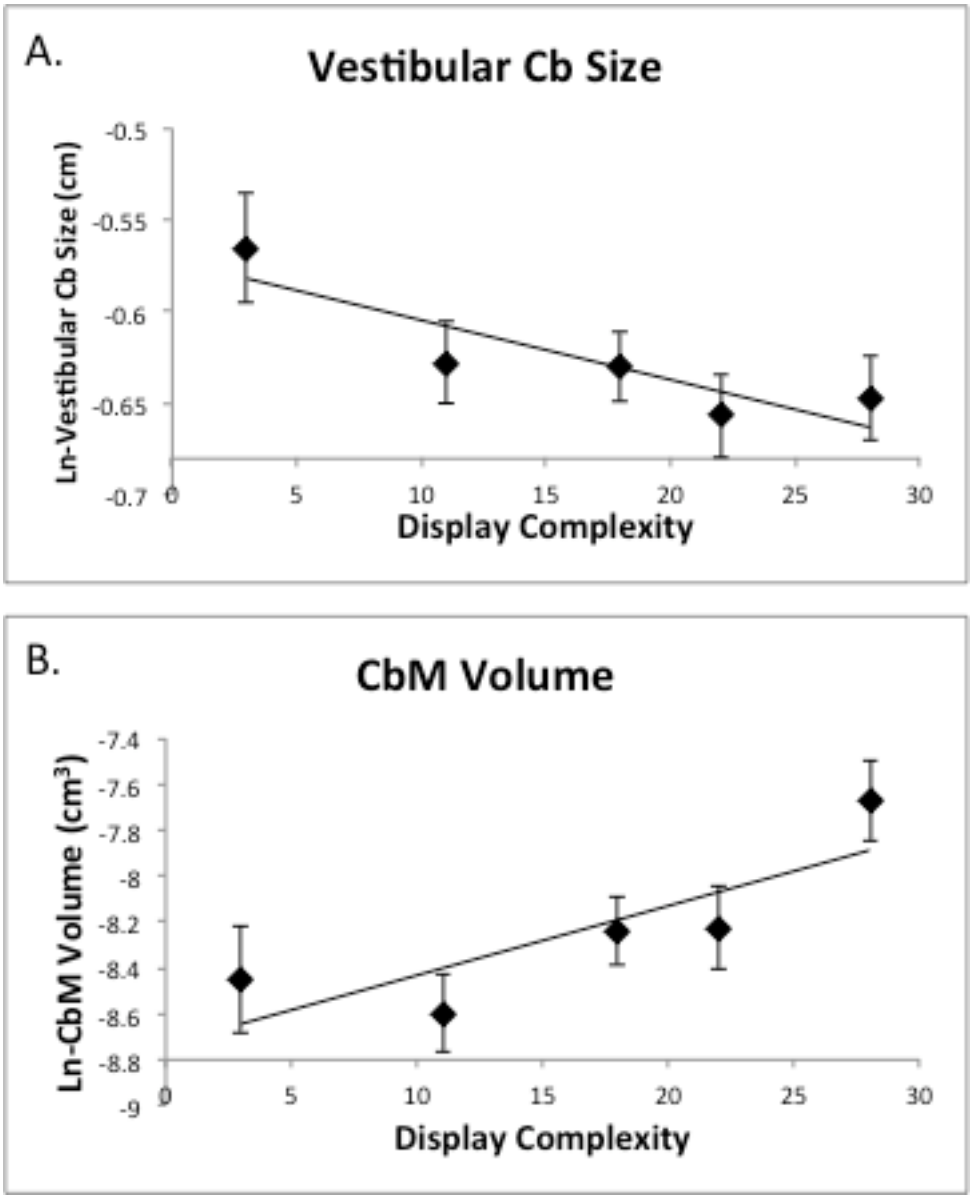

Figure 19. A) Linear regression of Vestibular Cb Size vs. Display Complexity. B) Linear regression of CbM Volume vs. Display Complexity. Both Vestibular Cb Size and CbM Volume were found to predict Display Complexity in a stepwise multiple regression. Standard error bars shown for each species, although they were not used in statistical analyses.

Phylogenetically corrected data showed similar results as for the non-corrected data. As required for independent contrasts analyses, linear regressions were forced through the origin. Results are summarized in Table 5.

Table 5. Results from phylogenetically corrected simple regressions of contrasts for each Cb morphology variable versus Display Complexity. The sign of the relationship is given for variables for which $p < 0.1$, highlighted in blue. These variables were then tested in a stepwise regression.

Cb Morphology Variable	r^2	p	slope
CbL Volume	0.000	0.983	
CbM Volume	0.688	0.083	pos.
CbL+CbM Volume	0.537	0.159	
CbL Cell Density	0.140	0.536	
CbM Cell Density	0.556	0.148	
CbL+CbM Cell Density	0.303	0.336	
CbL # Cells	0.213	0.434	
CbM # Cells	0.001	0.964	
CbL+CbM # Cells	0.071	0.666	
Cb Volume	0.279	0.360	
White Matter	0.809	0.038	pos.
Molecular Layer	0.620	0.114	
Granule Layer	0.050	0.717	
PC Layer Length	0.511	0.175	
Anterior Cb Size	0.006	0.905	
Posterior Cb Size	0.167	0.495	
Vestibular Cb Size	0.749	0.058	neg.
PC Size	0.685	0.084	neg.
PC Density	0.121	0.567	
PC #	0.001	0.955	
Vestibular Cb PC Size	0.082	0.640	
Vestibular Cb PC Density	0.028	0.787	
Vestibular Cb PC #	0.111	0.583	

Variables in Table 5 for which $p < 0.1$—the same variables as in non-corrected analyses (Table 4): CbM Volume, White Matter Volume, Vestibular Cb Size, and PC Size—were then tested in a stepwise multiple regression with entry probability of F set at 0.05

and removal probability of F set at 0.1. The significant model included only White Matter Volume ($F_{(1,4)}$ = 12.745, R^2_{adj}=0.746, p=0.038, B=48.2).

IV. DISCUSSION

The acrobatic courtship displays of manakins require coordination and planning of complex motor sequences. The substantial interspecific variation in display complexity allows one to compare the morphology of the Cb, a motor-planning region, across species to examine how the Cb functions in the performance of acrobatic displays. This system provides a novel perspective for studying the function and evolution of the Cb, a homologous structure found throughout vertebrates. Several Cb morphological variables were tested for an association with courtship display complexity. I hypothesized that at least the major measures of Cb morphology—Cb Volume, PC size and density, and CbM and CbL volume and cell density—would increase with increasing display complexity since PC and CbM/L measurements reflect major functions and are convergence points for inputs and outputs in the Cb.

The phylogenetically corrected results suggest a significant positive relationship between White Matter Volume and Display Complexity. That is, species that perform more complex displays have more white matter within the Cb. An increase in white matter would suggest an increase in the number of projections into and out of the Cb and Cb cortex. No other variables in this analysis were found to relate to Display Complexity despite the potential relatedness of many of the variables with white matter. The white matter consists of axons of PCs, cells in CbM and CbL, and cells located outside the Cb. Either there was not enough power in this analysis to detect other relationships or the white matter largely

originates from cells outside the Cb. Future studies could additionally examine the size of the Cb peduncles. This could be done by estimating the area in the transverse plane of each peduncle at the narrowest point on its path into the Cb. Focusing on the peduncles would provide information on all inputs and outputs to the Cb and would not include connections between the Cb nuclei and cortex.

Because the relationships did not seem to change substantially between the phylogenetically corrected and non-corrected analyses, and n was reduced from 5 to 4 with phylogenetic corrections, there is a possibility that differences in the stepwise regression results between the corrected and non-corrected data were affected by reduced statistical power. Therefore, the results of the non-phylogenetically corrected analyses should be interpreted along with that of the corrected data.

The model from the stepwise regression for non-corrected data consisted of a negative relationship between Vestibular Cb Size and a positive relationship between CbM Volume and Display Complexity. The increasing size of CbM Volume with Display Complexity indicates greater demand for processing by the Cb of motor information in more complex displays since the CbM projects to regions of the spinal cord and brainstem (Arends & Zeigler 1991). This result also suggests that Cb function related to display may be longitudinally organized because the Cb nuclei reflect parasagittal zones in the Cb cortex. Though few studies have specifically examined Cb nuclei size in relation to behavior, these data are consistent with the findings of Matano & Hirasaki (1997) regarding locomotor behavior in anthropoids. They found that CbL was enlarged relative to CbM in most species except in arboreal quadrupeds, which, like manakins, utilize both hind- and forelimbs to navigate a 3-dimensional environment. Arboreal quadrupeds had Cb

nuclei that were similar in development to one another, suggesting an increased demand for CbM function in arboreal quadrupeds relative to species with less complex locomotor types. The results for both CbM Volume and White Matter Volume support the hypothesis that regions of the Cb related to Display Complexity are larger due to increased processing demands as predicted by the principle of proper mass (Jerison 1973). However, the negative relationship reported here between Vestibular Cb Size and Display Complexity is contrary to this hypothesis.

Because the vestibular system contributes to balance and a sense of spatial orientation with respect to gravity, one would expect features of this system to be important in complex acrobatic displays. Hence, this negative relationship remains a mystery. The potential negative relationship between Vestibular Cb Size and Display Complexity could further be investigated by measuring the size of the vestibular nuclei in the brainstem. Because these nuclei receive inputs from the vestibular Cb, the size of these nuclei should also be inversely related to Display Complexity if there really is a reduction in vestibular processing with increased display complexity. If these nuclei are not inversely related to display, this could indicate that the results obtained in this study regarding the vestibular Cb do not reflect the true relationship and should be investigated in more species.

Strangely, PC Size trended toward a negative relationship with Display Complexity. In the simple regressions, this relationship had a p-value < 0.1, but PC Size did not reach significance in the stepwise regression. A decrease in PC size or density is associated with ataxia (D'Angelo 2009; Wolf et al. 1996; Andersen 2004), so one would not expect to see a decrease in PC size or density in manakin species with more complex acrobatic displays.

The prediction that Cb Volume would show a positive relationship with Display Complexity was not supported. Therefore, this relationship likely would remain absent even if other manakin species were included. Cb volume in males of five species of bowerbirds has been shown to be positively related to the complexity of the bower structure built by each species (Day et al. 2005). Building of a bower requires procedural learning, planning and performance of stereotyped postures and movements, so one also would have expected Cb Volume in manakins to relate to display complexity. However, a major difference between manakin and bowerbird courtship behaviors that could explain the discrepancy is that bower construction involves a high degree of manipulation of the environment. In both birds and mammals there is a correlation between Cb size and visual-guided manipulative skills (Sultan 2005; Sultan & Glickstein 2007), and the lack of manipulative skills involved in manakin displays could explain the lack of relationship of display with Cb size. Further support for this idea is that the golden-collared manakin (*M. vitellinus*), which removes forest litter in order to create a display arena, is the only manakin species in this study that manipulates its environment to a substantial degree, and *M. vitellinus* also has the largest Cb Volume.

Historically, Cb morphology, especially with regard to foliation patterns, has been described for species comparisons using only a single representative of each species with the implicit assumption that there is little to no intraspecific variation (Larsell 1967). However, in this study there was a remarkable amount of intraspecific variation in foliation patterns. Larsell (1967) mentioned that in a species of duck for which he examined at least two individuals, he noticed a difference in the number of subfolia, but few researchers have elaborated on this point or taken it into consideration when performing multispecies

studies. The substantial intraspecific variation in subfoliation, and even in basic foliation in one species, seen in the manakins suggests that even major morphological features of the Cb are not species specific, and confirms the necessity of including multiple individuals to represent a species in future research in this field. It also suggests that the assignment of functionality to specific folia cannot be done if foliation patterns themselves are not consistent.

There is evidence that this intraspecific variation in Cb morphology may reflect the size of the Cb. In a large comparative study including representative individuals of several avian orders, Cb volume predicted the degree of foliation, as measured using a standardized Cb foliation index (Iwaniuk et al. 2006a). Within the individuals in this study, which include three to four individuals per species within the same family (Pipridae) as well as two closely related flycatcher individuals, Cb volume significantly predicts the amount of Cb foliation as measured by a standardized foliation index. This is the first demonstration of such an effect at the family level.

A major limitation in this study was the limited access to brain tissue. Because these birds were wild caught, many months of work were required to obtain only a few individuals. Because fieldwork was done only in the Canal Zone of Panama, where the only manakin species present are those included in this study, it will be necessary to travel to new field sites to obtain different species. Given the amount of intraspecific variation present and the number of Cb morphology variables examined, it would help to include more individuals and more species in the future. However, because the results for Vestibular Cb Size and CbM Volume indicate such a strong significant relationship with Display Complexity despite low statistical power, it is likely that one or both of these

relationships would still be seen upon inclusion of more specimens. From museums, I have obtained eleven individuals representing six species of manakin and processed the brain tissue. These could not be included in this study due to major differences in tissue preparation between museum and fresh caught specimens as well as the amount of intraspecific variation. With the addition of more specimens, a separate parallel study of museum-prepared individuals could be performed. However, even though inclusion of more species will increase statistical power, the diversity of Cb functions could still interfere with the examination of the relationship of Cb morphology with display complexity.

The Cb has a wide variety of connections with the rest of the brain and the spinal cord and is involved in several types of behaviors. While it seems likely that the non-display behaviors of manakins are very similar, this is not necessarily the case. For example, subtle species differences in foraging behavior could exist. Certain species might prefer certain types of fruits that require different sallying behaviors, or species that live in more arid regions might rely on hunting insect prey more than species in strictly rainforest environments. Furthermore, if food is less localized for some populations, these populations will have larger home ranges and may even display in different lek locations throughout their lifetime. It is unknown how the Cb varies in relation to these potential variations in foraging and social behavior. It is also unknown whether manakin displays are learned, either fully or partially. Because bowerbirds learn how to build their bowers from watching others males, future research in bowerbirds should examine the size of CbL, which is thought to be related to cognition and motor planning, in relation to bower complexity.

In conclusion, the relationships determined in this study were a negative relationship for Vestibular Cb Size, a positive relationship for CbM Volume, and a positive relationship for White Matter Volume versus Display Complexity. The latter two results support my hypothesis and suggests that CbM's descending motor projections and the amount of neural communication in the Cb are related to the acrobatic nature of the displays. The negative relationship for Vestibular Cb Size contradicts my hypothesis and remains unexplained. Because non-phylogenetically corrected data produced relationships very similar to corrected data, species relatedness does not appear to confound the relationships in this study. Analyses of phylogenetically corrected data suggest that only White Matter Volume is positively related to Display Complexity, implying a greater number of inputs and outputs traversing the Cb in species with more complex displays. These findings suggest that there is correlated evolution of manakin display complexity and Cb morphology. Given the diversity of functions with which the Cb is involved, for the Cb to exhibit specializations specifically related to display, there likely is a strong selective force driving this correlated evolution. To further examine the strength of these findings, additional manakin species will be examined. Further research also should compare Cb morphology of males and females within species that perform complex displays. Because females do not display, Cb specializations should not be present.

LIST OF REFERENCES

Adrian ED (1943) Afferent areas in the cerebellum connected with the limbs. Brain 66:289-315.

Andersen BB (2004) Reduction of purkinje cell volume in cerebellum of alcoholics. Brain Research 1007:10-18.

Andersson G (1978) Climbing fiber microzones in cerebellar vermis and their projection to different groups of cells in the lateral vestibular nucleus. Experimental Brain Research 32:565-579.

Arends JJA, Zeigler HP (1991a) Organization of the cerebellum in the pigeon (columba livia): I. Corticonuclear and corticovestibular connections. The Journal of Comparative Neurology 306:221-244.

Arends JJA, Zeigler HP (1991b) Organization of the cerebellum in the pigeon (columba livia): II. Projections of the cerebellar nuclei. The Journal of Comparative Neurology 306:245-272.

Asanuma C (1983) Brainstem and spinal projections of the deep cerebellar nuclei in the monkey, with observations on the brainstem projections of the dorsal column nuclei. Brain Research Reviews 5:299-322.

Aylward EH, Habbak R, Warren AC, Pulsifer MB, Barta PE, Jerram M, Pearlson GD (1997) Cerebellar volume in adults with down syndrome. Archives of Neurology 54:209-212.

Bolk L (1904) Das cerebellum der saugetiere: Eine vergleichende anatomische untersuchung. Nederland Bydragen tot de Anatomie 3:1-136.

Bostwick KS (2003) High-speed video analysis of wing-snapping in two manakin clades (pipridae: Aves). Journal of Experimental Biology 206:3693-3706.

Bradbury JW (1981) The evolution of leks. In: Natural selection and social behavior (Alexander RD, Tinkle DW, eds), pp 138-169. New York: Chiron Press.

Brenowitz EA, Margoliash D, Nordeen KW (1997) An introduction to birdsong and the avian song system. Journal of Neurobiology 33:495-500.

Catania K, Kaas J (1995) Organization of the somatosensory cortex of the star-nosed mole. Journal of Comparative Neurology 351:549-567.

Chapman FM (1935) The courtship of gould's manakin (*manacus vitellinus vitellinus*) on barro colorado island, canal zone. Bulletin of The American Museum of Natural History 68:471-525

ChungSH, Marzban H, Hawkes R (2009) Compartmentation of the cerebellar nuclei of the mouse. Neuroscience 161:123-138.

Clarke PGH (1974) The organization of visual processing in the pigeon cerebellum. The Journal of Physiology 243:267-285.

Cleere N (1998) Nightjars: A guide to the nightjars, nighthawks, and their relatives. New Haven, CT: Yale University Press.

D'Angelo E, De Zeeuw CI (2009) Timing and plasticity in the cerebellum: Focus on the granular layer. Trends in Neurosciences 32:30-40.

Day LB (2003) The importance of hippocampus-dependent non-spatial tasks in analyses of homology and homoplasy. Brain Behavior and Evolution 62:96-107.

Day LB, Westcott DA, Olster DH (2005) Evolution of bower complexity and cerebellum size in bowerbirds. Brain Behavior and Evolution 66:62-72.

Day LB, Fusani L, Hernandez E, Billo TJ, Sheldon KS, Wise PM, Schlinger BA (2007) Testosterone and its effects on courtship in golden-collared manakins (*Manacus vitellinus*): Seasonal, sex, and age differences. Hormones and Behavior 51:69-76.

Devoogd TJ, Krebs JR, Healy SD, Purvis A (1993) Relations between song repertoire size and the volume of brain nuclei related to song: Comparative evolutionary analyses amongst oscine birds. Proceedings of the Royal Society of London B 254:75-82.

Duraes R, Loiselle B, Blake J (2007) Intersexual spatial relationships in a lekking species: Blue-crowned manakins and female hot spots. Behavioral Ecology 18:1029-1039.

DuVal EH (2007) Cooperative display and lekking behavior of the lance-tailed manakin (*Chiroxiphia lanceolata*). The Auk 124:1168-1185.

Ekerot CF (1979) The dorsal spino-olivocerebellar system in the cat. Ii. Somatotopical organization. Experimental Brain Research 36:219-232.

Feenders G, Liedvogel M, Rivas M, Zapka M, Horita H, Hara E, Wada K, Mouritsen H, Jarvis ED (2008) Molecular mapping of movement-associated areas in the avian brain: A motor theory for vocal learning origin. Plos One 3:1-27.

Fuentes CT, Bastian AJ (2007) 'motor cognition' - what is it and is the cerebellum involved? The Cerebellum 6:232-236.

Fusani L, Giordano M, Day LB, Schlinger BA (2007) High-speed video analysis reveals individual variability in the courtship displays of male golden-collared manakins. Ethology 113:964-972.

Garwicz M (1992) Distribution of cutaneous nociceptive and tactile climbing fibre input to sagittal zones in cat cerebellar anterior lobe. The European Journal of Neuroscience 4:289-295.

Ghez C, Thach WT (2000) The cerebellum. In: Principles of neural science (Kandel ER, Schwartz JH, Jessell TM, eds), p 837. New York: McGraw-Hill.

Glickstein M, Strata P, Voogd J (2009) Cerebellum: History. Neuroscience 162:549-559.

Gokcimen A, Ragbetli Me, Bas O, Tunc AT, Aslan H, Yazici AC, Kaplan S (2007) Effect of prenatal exposure to an anti-inflammatory drug on neuron number in cornu ammonis and dentate gyrus of the rat hippocampus: A stereological study. Brain Research 1127:185-192.

Gross NB (1970) Sensory representation withing the cerebellum of the pigeon. Brain Research 21:280-283.

Hook EB (1981) Down syndrome frequency in human populations and factors pertinent to variation in rates. In: Trisomy 21 (down syndrome): Research perspectives (de la Cruz FF, Gerald PS, eds), pp 3-68. Baltimore: University Park Press.

Iwaniuk AN, Hurd PL, Wylie DRW (2006a) The comparative morphology of the cerebellum in caprimulgiform birds: Evolutionary and functional implications. Brain Behavior and Evolution 67:53-68.

Iwaniuk AN, Hurd PL, Wylie DRW (2006b) Comparative morphology of the avian cerebellum: I. Degree of foliation. Brain Behavior and Evolution 68:45-62.

Iwaniuk AN, Hurd PL, Wylie DRW (2007) Comparative morphology of the avian cerebellum: Ii. Size of folia. Brain Behavior and Evolution 69:196-219.

Iwaniuk AN, Marzban H, Pakan JMP, Watanabe M, Hawkes R, Wylie DRW (2009) Compartmentation of the cerebellar cortex of hummingbirds (aves: Trochilidae) revealed by the expression of zebrin ii and phospholipase c-beta-4. Journal of Chemical Neuroanatomy 37:55-63.

Jerison HJ (1973) Evolution of the Brain and Intelligence: Academic Press. 482 pp.

Karten HJ, Hodos W (1967) A stereotaxic atlas of the brain of the pigeon (columba livia). Baltimore: Johns Hopkins Press. 193 pp.

Karten HJ, Finger TE (1976) A direct thalamo-cerebellar pathway in pigeon and catfish. Brain Research 120:335-338.

Lange W (1975) Cell number and cell density in the cerebellar cortex of man and some other mammals. Cell and Tissue Research 157:115-124-124.

Larsell O (1947) The development of the cerebellum in man in relation to its comparative anatomy. Journal of Comparative Neurology. 87:85-129.

Larsell O (1948) The development and subdivisions of the cerebellum of birds. Journal of Comparative Neurology 89:123-189.

Larsell O (1953) The cerebellum of the cat and the monkey. Journal of Comparative Neurology 99:135-199.

Larsell O (1967) The comparative anatomy and histology of the cerebellum: From myxinoids through birds. Minneapolis: University of Minnesota Press.

Lowenthal M, Horsley V (1897) On the relations between the cerebellar and other centres (namely cerebral and spinal) with especial reference to the action of antagonistic muscles. (preliminary account). Proceedings of the Royal Society of London 61:20-25.

Luciani L (1891) Il cervelletto; nuovi studi di fisiologia normale e patologica. Firenze: Le Monnier.

Maddison, W.P. & D.R. Maddison (2006). Mesquite: A modular system for evolutionary analysis. Version 2.72. http://mesquiteproject.org

Midford, P. E., T. Garland Jr., and W. P. Maddison (2005). PDAP Package of Mesquite. Version 1.15

Manni E, Petrosini L (2004) A century of cerebellar somatotopy: A debated representation. Nature Reviews Neuroscience 5:241-249.

Matano S, Hirasaki E (1997) Volumetric comparisons in the cerebellar complex of anthropoids, with special reference to locomotor types. American Journal of Physical Anthropology 103:173-183.

McKay BD, Barker FK, Mays Jr. HL, Doucet SM, Hill GE (2010) A molecular phylogenetic hypothesis for the manakins (Aves: Pipridae). Molecular Phylogenetics and Evolution 55:733.

Moran T, Richtsmeier J, Troncoso J, Reeves R (2000) Discovery and genetic localization of down syndrome cerebellar phenotypes using the ts65dn mouse. Human Molecular Genetics 9:195-202.

Necker R, Neumann V (1997) Response characteristics of the cerebellar nuclear cells in the pigeon. NeuroReport 8:1485-1489.

Nixdorf-Bergweiler BE, Bischof H (2007) A stereotaxic atlas of the brain of the zebra finch, taeniopygia guttata, with special emphasis on telencephalic visual and song system nuclei in transverse and sagittal sections. Bethesda: National Library of Medicine, NCBI Bookshelf.

Nottebohm F, Arnold AP (1976) Sexual dimorphism in vocal control areas of the songbird brain. Science 194:211-213.

Pagano G (1904) Saggio di localizzazione cerebellare. Rivista di Patologia Nervosa a Mental 9:209-228.

Pakan JMP, Iwaniuk AN, Wylie DRW, Hawkes R, Marzban H (2007) Purkinje cell compartmentation as revealed by zebrin ii expression in the cerebellar cortex of pigeons (*Columba livia*). Journal of Comparative Neurology 501:619-630.

Pakan JMP, Graham DJ, Iwaniuk AN, Wylie DRW (2008) Differential projections from the vestibular nuclei to the flocculus and uvula-nodulus in pigeons (*Columba livia*). Journal of Comparative Neurology 508:402-417.

Paxinos G, Carrive P, Wang H, Wang P (1999) Chemoarchitectonic atlas of the rat brainstem. San Diego: Academic Press.

Person AL, Gale SD, Farries MA, Perkel DJ (2008) Organization of the songbird basal ganglia, including area X. The Journal of Comparative Neurology 508:840-866.

Prum R (1994) Phylogenetic analysis of the evolution of alternative social-behavior in the manakins (aves, pipridae). Evolution 48:1657-1675.

Prum R (1998) Sexual selection and the evolution of mechanical sound production in manakins (aves : Pipridae). Animal Behaviour 55:977-994.

Prum RO (1990) Phylogenetic analysis of the evolution of display behavior in the neotropical manakins (aves: Pipridae). Ethology 84:202-231.

Rosen GD, Harry JD (1990) Brain volume estimation from serial section measurements - a comparison of methodologies. Journal of Neuroscience Methods 35:115-124.

Schlinger BA, Schultz JD, Hertel F (2001) Neuromuscular and endocrine control of an avian courtship behavior. Hormones and Behavior 40:276-280.

Schlinger BA, Day LB, Fusani L (2008) Behavior, natural history and neuroendocrinology of a tropical bird. General and Comparative Endocrinology 157:254-258.

Schmit C, Hof PR (2000) Recommendations for straightforward and rigorous methods of counting neurons based on a computer simulation approach. Journal of Chemical Neuroanatomy 20:93-114.

Schulte M, Necker R (1998) Processing of spinal somatosensory information in anterior and posterior cerebellum of the pigeon. Journal of Comparative Physiology A 183:111-120.

Schultz JD, Fusani L, Hau M, and Schlinger B, submitted. Androgen receptor expression in motor and sensory neurons innervating limb muscles of the golden-collared manakin, a bird with an acrobatic courtship display.

Schwarz DWF, Schwarz IE (1986) Projections of afferents from individual vestibular sense organs to the vestibular nuclei in the pigeon. Acta Otolaryngologica 102:463-473.

Sherrington CS (1897) Double (antidrome) conduction in the central nervous system. Proceedings of the Royal Society of London 61:243-246.

Sherry DF, Jacobs LF, Gaulin SJC (1992) Spatial memory and adaptive specialization of the hippocampus. Trends in Neurosciences 15:298-303.

Skutch AF (1969) Life histories of Central American birds III: Families Cotingidae, Pipridae, Formicariidae, Furnariidae, Dendrocolaptidae, and Picidae. Berkeley: Cooper Ornithological Society.

Snider RS (1944a) Receiving areas of the tactile, auditory, and visual systems in the cerebellum. Journal of Neurophysiology 7:331.

Snider RS (1944) Receiving areas of the tactile, auditory, and visual systems in the cerebellum. Journal of Neurophysiology. 7:331-357.

Steinlin M (2008) Cerebellar disorders in childhood: Cognitive problems. Cerebellum (London, England) 7:607-610.

Stoodley CJ, Valera EM, Schmahmann JD (2010) An fmri study of intra-individual functional topography in the human cerebellum. Behavioural Neurology 23:65-79.

Sugihara I, Shinoda Y (2007) Molecular, topographic, and functional organization of the cerebellar nuclei: Analysis by three-dimensional mapping of the olivonuclear projection and aldolase c labeling. The Journal of Neuroscience 27:9696-9710.

Sultan F (2005) Why some bird brains are larger than others. Current Biology 15:R649-R650.

Sultan F, Glickstein M (2007) The cerebellum: Comparative and animal studies. Cerebellum 6:168-176.

Szekely T, Catchpole CK, Devoogd A, Marchl Z, Devoogd TJ (1996) Evolutionary changes in a song control area of the brain (HVC) are associated with evolutionary changes in song repertoire among european warblers (Sylviidae). Proceedings of the Royal Society of London B 263:607-610.

Torriero S, Oliveri M, Giacomo K, Caltagirone C, Petrosini L (2007) The what and how of observational learning. Journal of Cognitive Neuroscience 19:1656-1663.

Tran KD, Smutzer G, Doty R, Arnold S (1998) Reduced purkinje cell size in the cerebellar vermis of elderly patients with schizophrenia. The American Journal of Psychiatry 155:1288-1290.

Trott R (1987) The cerebellar corticonuclear projection from lobule vb/c of the cat anterior lobe: A combined electrophysiological and autoradiographic study I. Projections from the intermediate region. Experimental Brain Research 66:318-338.

Trott R, Armstrong D (1987) The cerebellar corticonuclear projection from lobule vb/c of the cat anterior lobe: A combined electrophysiological and autoradiographic study II. Projections from the vermis. Experimental Brain Besearch 68:339-354.

Van Kan PL (1993) Output organization of intermediate cerebellum of the monkey. Journal of Neurophysiology 69:57-73.

Watson RE, Wiegand SJ, Clough RW, Hoffman GE Use of cryoprotectant to maintain long-term peptide immunoreactivity and tissue morphology. Peptides 7:155-159.

West GB, Brown JH, Enquist BJ (1997) A general model for the origin of allometric scaling laws in biology. Science 276:122-126.

Westcott DA (1994) Behavior and social organization during the breeding season in *Mionectes oleagineus*, a lekking flycatcher. The Condor 96:672.

Whitlock DG (1952) A neurohistological and neurophysiological study of afferent fiber tracts and receptive areas of the avian cerebellum. The Journal of Comparative Neurology 97:567-635.

Wild J (1992) Direct and indirect "Cortico"-rubral and rubro-cerebellar cortical projections in the pigeon. Journal of Comparative Neurology 326:623-636.

Wild JM, Williams MN (2000) A direct cerebrocerebellar projection in adult birds and rats. Neuroscience 96:333-339.

Wolf LW, LaRegina MC, Tolbert DL (1996) A behavioral study of the development of hereditary cerebellar ataxia in the shaker rat mutant. Behavioural Brain Research 75:67-81.

Zusi RL, Bentz GD (1984) Myology of the purple-throated carib (*Eulampis jugularis*) and other hummingbirds (Aves: Trochilidae). Smithsonian Contributions to Zoology 385:1-70.

VITA

Steven Wilkening attended Cornell University, College of Arts and Sciences, in Ithaca, NY from August 2004 to May 2008 and graduated with a Bachelor of Arts degree in Biology. He entered the Master's program at The University of Mississippi, Oxford, MS in August 2008.